

Accepted to ApJ

Identifying the young low-mass stars within 25 pc. II. Distances, kinematics & group membership¹

Evgenya L. Shkolnik

Lowell Observatory, 1400 W. Mars Hill Road, Flagstaff, AZ 86001

shkolnik@lowell.edu

Guillem Anglada-Escudé

Universität Göttingen, Institut für Astrophysik, Friedrich-Hund-Platz 1, 37077 Göttingen, Germany

Michael C. Liu, Brendan P. Bowler

*Institute for Astronomy, University of Hawaii at Manoa
2680 Woodlawn Drive, Honolulu, HI 96822*

Alycia J. Weinberger, Alan P. Boss

Department of Terrestrial Magnetism, Carnegie Institution of Washington, 5241 Broad Branch Road, NW, Washington, DC 20015

I. Neill Reid

Space Telescope Science Institute, Baltimore, MD 21218

and

Motohide Tamura

National Astronomical Observatory of Japan, Tokyo, Japan

¹Based on observations collected at the W. M. Keck Observatory, the Canada-France-Hawaii Telescope, the du Pont Telescope at Las Campanas Observatory, and the Subaru Telescope. The Keck Observatory is operated as a scientific partnership between the California Institute of Technology, the University of California, and NASA, and was made possible by the generous financial support of the W. M. Keck Foundation. The CFHT is operated by the National Research Council of Canada, the Centre National de la Recherche Scientifique of France, and the University of Hawaii.

ABSTRACT

We have conducted a kinematic study of 165 young M dwarfs with ages of $\lesssim 300$ Myr. Our sample is composed of stars and brown dwarfs with spectral types ranging from K7 to L0, detected by *ROSAT* and with photometric distances of $\lesssim 25$ pc assuming the stars are single and on the main-sequence. In order to find stars kinematically linked to known young moving groups (YMGs), we measured radial velocities for the complete sample with Keck and CFHT optical spectroscopy and trigonometric parallaxes for 75 of the M dwarfs with the CAPSCam instrument on the du Pont 2.5-m Telescope. Due to their youthful overluminosity and unresolved binarity, the original photometric distances for our sample underestimated the distances by 70% on average, excluding two extremely young ($\lesssim 3$ Myr) objects found to have distances beyond a few hundred parsecs. We searched for kinematic matches to 14 reported YMGs and identified 9 new members of the AB Dor YMG and 2 of the Ursa Majoris group. Additional possible candidates include 6 Castor, 4 Ursa Majoris, 2 AB Dor members, and 1 member each of the Her-Lyr and β Pic groups. Our sample also contains 27 young low-mass stars and 4 brown dwarfs with ages $\lesssim 150$ Myr which are not associated with any known YMG. We identified an additional 15 stars which are kinematic matches to one of the YMGs, but the ages from spectroscopic diagnostics and/or the positions on the sky do not match. These warn against grouping stars together based only on kinematics and that a confluence of evidence is required to claim that a group of stars originated from the same star-forming event.

Subject headings: Stars: late-type, ages, associations, parallaxes, radial velocities
– Surveys: X-ray – Galaxy: solar neighborhood

1. Introduction

Planet-formation studies require a range of stellar host mass and age in order to test models of planet and disk evolution. The vast majority of confirmed exoplanets are in systems greater than 1 Gyr old, and efforts to find the youngest planets, those just forming in their disks around T Tauri stars (1 – 3 Myr old), are just beginning (Prato et al. 2008; Crockett et al. 2011; Kraus & Ireland 2011). Young stars with ages spanning 10 to 100 Myr fill a particularly interesting, and relatively unexplored, gap as this time scale coincides with the end of giant planet formation (e.g. Boss 2011) and the onset of active terrestrial planet formation.

From an observational perspective, this time range is critical for direct imaging searches of planets and disks (e.g. Marois et al. 2008; Liu et al. 2010). Planets cool and fade dramatically during this period, e.g. the luminosity of a $5\text{-}M_{Jup}$ planet drops by 2 – 3 orders of magnitude in this time span and its effective temperature decreases from 1300 K to 400 K (Baraffe et al. 2003). Also in this time period, the fraction of debris disks around AFGK main-sequence stars decreases significantly (e.g. Rieke et al. 2005; Hillenbrand et al. 2008). These attributes have made young, nearby stars prime targets at direct imaging searches for exoplanets and circumstellar disks, as supported by the imaged planets around the 10 – 30-Myr stars β Pic and HR 8799 (Lagrange et al. 2010; Marois et al. 2008).

M dwarfs offer an additional observational advantage. Their intrinsic faintness provides a more favorable contrast in star-planet flux, aiding the detection of faint planetary-mass companions. M dwarfs also dominate the stellar mass function by number: roughly 3 out of 4 stars in a volume-limited sample of the solar neighborhood are M dwarfs (Reid et al. 1995; Bochanski et al. 2010). So in principle low-mass stars could represent the most common and nearest hosts of planetary systems, providing a much larger population of targets for direct imaging of exoplanets than has been studied to date.

Searches for young low-mass stars have been carried out using X-ray (e.g. Jeffries 1995; Webb et al. 1999; Montes et al. 2001; Shkolnik et al. 2009, SLR09 hereafter) and UV (Shkolnik et al. 2011; Rodriguez et al. 2011) surveys to identify strong coronal and chromospheric emission. SLR09 and Shkolnik et al. (2011) estimated that M dwarfs with fractional X-ray and UV luminosities of $\log(F_X/F_J) > -2.5$ and $\log(F_{NUV}/F_J) > -4$ are younger than ~ 300 Myr, based on comparisons with Pleiades (120 Myr) and Hyades (625 Myr) members. However, determining a more accurate age for an individual star is more difficult.

Over the past decade, many dispersed young stars have been kinematically linked to coeval moving groups (e.g., Zuckerman & Song 2004; Torres et al. 2008, and references therein), for which more accurate ages are available through comparison of the bulk group properties with stellar isochrones and lithium-depletion models (e.g. Soderblom 2010). Thus, pinning an X-ray- or UV- bright M dwarf to one of the known young moving groups (YMGs) provides a more accurate means to determine its age.

The current census of YMG members is mostly limited to AFGK-type stars due to the past reliance on optical catalogs for distances and proper motions, e.g., the Hipparcos and Tycho catalogs (Perryman & ESA 1997), which exclude most of the fainter nearby M dwarfs. If the initial mass function of YMGs follows the field, we can expect that there are many unidentified low-mass members of the known YMGs, e.g. ≈ 60 M dwarfs missing from the β Pic YMG and ≈ 20 mid-Ms from the TW Hydrae Association (Shkolnik et al. 2011). Recent searches for these low-mass members using large photometric and proper motion

catalogs have found many candidates awaiting confirmation with follow-up parallaxes and radial velocities (e.g., Lépine & Simon 2009; Schlieder et al. 2012).

This paper presents the kinematic analysis of the 165 young M dwarfs first described in SLR09,¹ including radial velocities (RVs) for all the targets, trigonometric parallaxes for half the sample, and three-dimensional space motions with the goal of providing more accurate ages by linking these stars to known YMGs.

2. The Sample

Our original sample of nearby low-mass stars was drawn from the NStars census (Reid et al. 2003, 2004) and the Moving-M sample (Reid et al. 2007b), which contained ≈ 1100 M dwarfs. Distances were mainly available through spectrophotometric relations as only 11% had parallaxes. We limited the sample to a photometric distance of 25 pc assuming the stars are single and on the main sequence (e.g., Reid & Cruz 2002; Cruz et al. 2003). This sample was cross-matched with the *ROSAT* All-Sky Survey Bright Source Catalog and Faint Source Catalog (Voges et al. 1999, 2000) as X-ray activity is a powerful indicator of youth (e.g. Preibisch & Feigelson 2005). Target stars were chosen to have high X-ray emission ($\log(F_X/F_J) > -2.5$) comparable to or greater than that of Pleiades members (120 Myr, Stauffer et al. 1998). A more detailed description of the sample selection process can be found in SLR09, where we used high-resolution optical spectra to determine spectral types (SpT) and eliminate spectroscopic binaries (SB; Shkolnik et al. 2010). We used spectroscopic age diagnostics such as low surface gravity, $H\alpha$ emission and lithium absorption to provide upper and lower age limits for each of the targets.

3. The Radial Velocities

We acquired high-resolution échelle spectra of 155 (of the 165) young M dwarfs in the SLR09 sample with the High Resolution Échelle Spectrometer (HIRES; Vogt et al. 1994) on the Keck I 10-m telescope and with the Échelle SpectroPolarimetric Device for the Observation of Stars (ESPaDOnS; Donati et al. 2006) on the Canada-France-Hawaii 3.6-m telescope, both located on the summit of Mauna Kea. These spectra were first described in SLR09.

¹There are 10 additional stars in this paper compared to SLR09, including 8 common proper-motion companions found during the CAPSCam astrometric observations and 2 young M dwarfs observed in support of the Gemini NICI Planet-Finding Campaign (Liu et al. 2010).

We used the 0.861" slit with HIRES to give a spectral resolution of $\lambda/\Delta\lambda \approx 58,000$. The detector consists of a mosaic of three 2048×4096 15- μm pixel CCDs, corresponding to a blue, green and red chip spanning 4900 – 9300 Å. To maximize the throughput near the peak of a M dwarf spectral energy distribution, we used the GG475 filter with the red cross-disperser.

ESPaDOnS is fiber fed from the Cassegrain to Coudé focus where the fiber image is projected onto a Bowen-Walraven slicer at the spectrograph entrance. With a 2048×4608 -pixel CCD detector, ESPaDOnS' 'star+sky' mode records the full spectrum over 40 grating orders covering 3700 to 10400 Å at a spectral resolution of $\lambda/\Delta\lambda \approx 68,000$. The data were reduced using *Libre-ESpRIT*, a fully automated reduction package provided for the instrument and described in detail by Donati et al. (1997, 2007).

Each stellar exposure was bias-subtracted and flat-fielded for pixel-to-pixel sensitivity variations. After optimal extraction, the 1-D spectra were wavelength calibrated with a Th-Ar arc. Finally the spectra were divided by a flat-field response curve and corrected to the heliocentric velocity. The final spectra were of moderate S/N, reaching 20 – 50 per pixel at 7000 Å. Each night, spectra were also taken of an A0V standard star for telluric correction and an early-, mid-, and/or late-M RV standard.²

We cross-correlated each of 7 orders between 7000 and 9000 Å of each stellar spectrum with an RV standard of similar spectral type using the *fxcor* routine (Fitzpatrick 1993) in IRAF.³ We measure the RVs from the gaussian peaks fitted to the cross-correlation function, taking the average and RMS of all orders as the final measurements. The RMS was typically less than 1 km s⁻¹ for both instruments. (Multi-lined spectroscopic binaries were removed from the sample and reported in Shkolnik et al. 2010.) The RVs, SpTs and other relevant information for each target are listed in Table 1.

4. Astrometric Observations

We measured parallaxes for the 75 targets (45% of our sample) observable with the CAPSCam instrument mounted on the 2.5-m du Pont Telescope at Las Campanas Observatory. An additional 8 stars had published parallaxes. CAPSCam was specifically designed

²See Table 3 of SLR09 for the list of RV standards used.

³IRAF (Image Reduction and Analysis Facility) is distributed by the National Optical Astronomy Observatories, which is operated by the Association of Universities for Research in Astronomy, Inc. (AURA) under cooperative agreement with the National Science Foundation.

for high-accuracy astrometry of M dwarfs in a bandpass covering $8000 \text{ \AA} - 9000 \text{ \AA}$. Its pixel size is $0.1956''$ with a field of view of $6.63' \times 6.63'$. Since the stars in this program are relatively bright ($I = 9 - 12 \text{ mag}$), we used the guide window to obtain short integrations of 0.5 to 1 sec. while exposing the full field of view for 30 to 60 sec. We used this instrument to obtain between 3 and 6 astrometric epochs on each of 75 targets, with a minimum time baseline of 1.5 years. The astrometric analysis was performed with the ATPa software developed in the framework of the Carnegie Astrometric Planet Search Program (CAPS). A more detailed description of the data analysis techniques can be found in Boss et al. (2009) and Anglada-Escudé et al. (2011).

In order to measure the parallax, one has to measure the motion of a star with respect to background sources. The motion on a local tangent plane to the sky is modeled using the 5 astrometric observables: R.A. and Dec. of the initial positions (α_0 and δ_0), proper motion in R.A. and Dec. (μ_α and μ_δ) and parallax (π). The local tangent plane formalism is outlined in the Hipparcos catalog reference guide (Perryman & ESA 1997) where the motion of a star is given by

$$X = \alpha_0 + \mu_\alpha (t - t_0) - \pi p_\alpha [t] \quad (1)$$

$$Y = \delta_0 + \mu_\delta (t - t_0) - \pi p_\delta [t] \quad (2)$$

where p_α and p_δ are the so-called parallax factors which are the projected motion of a star with $\pi = 1$ on the tangent plane of the sky defined by R.A. and Dec. positions, X and Y , respectively. The reference epoch t_0 implicitly defines the time against which all the quantities are referenced, and in our case, we use the last epoch of the observations.

In order to measure the motion of a star with respect to the background objects, the field distortions of each image first need to be calibrated. To do this, a subset of stable reference stars are used to fit a 2-d polynomial to each image. Given the measured local plane position x_i^{obs} and y_i^{obs} of each star on the detector in pixel coordinates, the calibrated position X_i and Y_i should be

$$X = a_0 + a_x x + a_y y + a_{xx} x^2 + a_{yy} y^2 + a_{xy} xy + \dots \quad (3)$$

$$Y = b_0 + b_x x + b_y y + b_{xx} x^2 + b_{yy} y^2 + b_{xy} xy + \dots \quad (4)$$

where the a and b coefficients need to be determined for each image. For this program, we used a second order distortion (terms up to x^2 , y^2 and xy) which required fitting 6

coefficients for each axis. This means that, at the very least, 6 reference stars are required for each field on each image. We used ≥ 10 reference stars in each field. Note that the absolute field geometry and the positions of the reference stars are not known a priori with enough accuracy. Because of this, the fitting process is iterative. In a first iteration, the nominal positions X and Y of all the stars are taken from a high quality image and all the other images are matched to it. Then an astrometric solution fit is obtained and a refined catalog of source positions, proper motions and parallaxes is generated. Those stars showing smaller residuals are used as the references in the following iterations. As a result, the astrometric solution for the target, as well as for all the other stars in the field, is obtained. This process is iterated between 3 to 5 times until convergence is reached (i.e. when the RMS improves less than 0.1 mas from one iteration to the next). After the fitting procedure, a typical target star has an RMS between 0.6 and 1.5 mas/epoch.

All the processing is done using the ATPa software specifically developed for CAPSCam. The software controls the end-to-end processing, which consists of centroid and source extraction, crossmatching, distortion, and calibration, producing final astrometric products. These products are source catalogs with the astrometric solutions and the motion of each star in the field. From measurements on many other fields within the CAPS project (Boss et al. 2009), the absolute orientation of CAPSCam is known to be stable down to 10' RMS in position angle (X is East-West, Y is North-South). In the small angle approximation, this angle, 0.0029 radians, is the maximum relative systematic error induced on any measured small offset. This is, all measured displacements (e.g. due to parallax and proper motion) contain a relative uncertainty of 0.3% due the unknown absolute field rotation. The plate scale has also been measured to be constant at 0.5% precision so both effects added in quadrature amounts to 0.6%. Given that this is significantly smaller than our aimed precision of the parallaxes (5%), nominal orientation and scale of CAPSCam were assumed for all the fields and the associated uncertainties were not included in the error budget for the distance determinations.

In addition to the astrometric parameters, the pipeline also provides a Monte Carlo estimate of the uncertainties. This is important when the number of independent measurements (twice the number of epochs because each measurement is two dimensional) is similar to the number of unknowns (i.e. ~ 5 astrometric parameters). The formal uncertainties derived from the equivalent least squares problem are typically too optimistic in this situation. Instead, we simulated 1000 datasets evaluated at the same epochs of observation and added Gaussian noise with an empirically determined uncertainty on each direction. The epoch uncertainty is estimated by computing the standard deviation of the residuals of the reference stars over all the epochs (not individual images). From other CAPSCam programs (e.g. Boss et al. 2009), we know that the typical uncertainty for 20 minutes on sky integration is

usually better than 1.5 mas. When the standard deviation obtained from the references is lower than this typical precision, we conservatively assume a single epoch uncertainty of 1.5 mas. This procedure allowed us to obtain realistic uncertainties and account for parameter correlation (e.g. proper motion and parallax) robustly. Note that this is an approximate but conservative approach because it assumes the same empirically determined uncertainty on all the epochs, even if there is a very poor quality one contaminating the measure of the uncertainty. Given the low number of observations compared to the free parameters and because astrometric measurements tend to be dominated by epoch-to-epoch systematic effects, we consider that this Monte Carlo approach provides the most secure and reliable estimation of the uncertainties in the astrometric observables.

In several instances, the RMS of the residuals of the target star is significantly larger than expected, e.g. ~ 4 mas RMS, when a typical star in the same field has 1.6 mas RMS. We found this occurs when the target appears to be a barely resolved visual binary (VB) with a separation smaller than $1.5''$. In these cases, we assigned a more conservative 5-mas uncertainty to the parallax measurement. There are a few stars with excess scatter but no evidence for binarity. All the barely-resolved binaries and high-RMS stars are flagged in Table 2.

The last important issue is that parallax measurements are made relative to the reference stars. The reference stars are not at an infinite distance and thus have a finite parallactic motion as well. Because of the matching process in the geometric calibration step (Equations 3 and 4), the average parallactic motion of the references will be absorbed so there will be a zero-point ambiguity in the measurement of the distance to the target. Correcting for the zero-point parallax requires making an educated guess of the distances to the reference stars, which may be complicated by the fact that good homogeneous photometry is not available in all cases. Instead, we estimated the typical zero-point correction to a few fields and applied it to the rest of the dataset. This procedure consists of using the photometry in the NOMAD catalog (B, J, H and K), estimating the photometric distance to a few reference stars, and computing the average difference between the measured parallax and the photometric one. Further details on the zero-point correction computation can be found in Anglada-Escudé et al. (2011). In the fields we tested, the zero-point correction was found to be smaller than 1 mas in all cases, with an average value of approximately +0.5 mas. Given that the precision in the relative parallax is never better than 1 mas, we add in quadrature the 0.5 mas obtained from the test fields to their statistical uncertainties of the measured parallaxes. Note that our typical target lies within 30 pc ($\pi=33$ mas), meaning that a 0.5-mas uncertainty represents only a 2% systematic error in the actual distance (compared to the 1.5 mas or 5% contribution derived from typical random errors in the measured relative parallaxes.)

Table 2 gives an overview of the quality of the raw astrometric measurements. In 11 cases, we can compare our trigonometric distances with those in the literature. As seen in Figure 1 and Table 3, the agreement is fairly good, typically well within 1- σ level error bar, indicating that we have been conservative in our uncertainty estimates. The RMS of the differences is 1.6 pc or 10% relative error with a $\tilde{\chi}^2$ of 0.888 (8 degrees of freedom). The color-magnitude-diagram (CMD) of the stars with parallaxes is shown in Figure 2 where more than two-thirds of the stars lie above the 300 Myr isochrone (Baraffe et al. 1998), consistent with their overluminosity due to young ages. The age distribution of our sample is shown in Figure 3.

5. Stellar Kinematics

We use our RV measurements in conjunction with the star’s distance and proper motions to measure the 3-dimensional space velocity (UVW), with U positive in the direction of the Galactic center, V positive in the direction of Galactic rotation, and W positive in the direction of the North Galactic Pole. This provides a way to refine stellar ages by linking stars kinematically to known YMGs and associations. However, as discussed below, kinematics alone are not sufficient to assign group membership.

5.1. UVW Space Velocities

The heliocentric velocities of the stars in Galactic coordinates and their uncertainties were computed using the prescriptions given by Johnson & Soderblom (1987). In order to find the best kinematic match to a YMG we evaluated the following reduced $\tilde{\chi}^2$ statistic with 3 degrees of freedom:

$$\tilde{\chi}^2 = \frac{1}{3} \left[\frac{(U_* - U_{MG})^2}{(\sigma_{U_*}^2 + \sigma_{U,MG}^2)} + \frac{(V_* - V_{MG})^2}{(\sigma_{V_*}^2 + \sigma_{V,MG}^2)} + \frac{(W_* - W_{MG})^2}{(\sigma_{W_*}^2 + \sigma_{W,MG}^2)} \right] \quad (5)$$

where U_* , V_* and W_* are the components of the heliocentric velocity of the star in Galactic coordinates and U_{MG} , V_{MG} and W_{MG} are the average components of the heliocentric velocity of the moving group (MG). σ_{U_*} , σ_{V_*} and σ_{W_*} are the measurement uncertainties derived from the observations and $\sigma_{U,MG}$, $\sigma_{V,MG}$ and $\sigma_{W,MG}$ are the internal velocity scatter (i.e. standard deviation of the velocities) of a given YMG.

This $\tilde{\chi}^2$ is a merit function that should be close to 1 if the UVW of the star and the

UVW of the YMG coincide at $1\text{-}\sigma$ level in all 3 velocity components. We accept stars as kinematic matches if $\tilde{\chi}^2 < 9$. Such a threshold ensures that we will recover 97% of the possible members of a sample of stars. We note that moving groups with large internal velocity scatter will be favored if a star has a similar UVW match to two associations. For matching purposes and to avoid over-weighting associations with large intrinsic scatters, we assume $\sigma_{U,MG} = \sigma_{V,MG} = \sigma_{W,MG} = 2 \text{ km s}^{-1}$, corresponding to what is typically 1σ of the velocity dispersion reported for the YMGs. Also, to avoid making wrong matches for stars with large UVW uncertainties, we only accept matches when the velocity modulus ($\Delta v = \sqrt{(U_* - U_{MG})^2 + (V_* - V_{MG})^2 + (W_* - W_{MG})^2}$), a measure of the difference between the UVW of a star and the UVW of a moving group, is less than 8 km s^{-1} . We chose an 8-km s^{-1} limit in 3-dimensional velocity space in order to find all possible matches assuming a $\approx 2 \text{ km s}^{-1}$ velocity dispersion in each of U , V and W of the YMG members. Because the vast majority of the known YMG members fall within these $\tilde{\chi}^2$ and velocity modulus limits (Figure 4), we further refine our criteria to $\Delta v < 5 \text{ km s}^{-1}$ and $\tilde{\chi}^2 < 6$ to identify the most probable members. These limits were set by the Δv and $\tilde{\chi}^2$ distributions of the known YMG members of which 90% lie within these limits (Figure 4).

Eighty-three of our targets have trigonometric parallaxes. For these, the UVW s are more precise than stars that do not have parallaxes. For the remaining targets, we calculated photometric distances using the Baraffe et al. (1998) solar-metallicity models. Our input data were effective temperatures using the Leggett et al. (2000) and Leggett et al. (2001) conversions from spectral types, 2MASS K_s magnitudes, and the upper and lower age limits determined from the spectroscopy and X-ray emission (SLR09). The mean photometric distances are reported in Table 1 with uncertainties spanning the full age range. Photometric distances are also corrected for any known binaries unresolved in the catalog photometry, either found during the spectroscopic and/or parallax programs described here or from adaptive optics imaging of these objects by Bowler et al. (in preparation and see Section 6).

A comparison of the trigonometric distances with the photometric distances corrected for youth (using the upper age limits from the spectroscopic diagnostics) and resolved binaries is shown in Figure 5. Excluding the two very young stars at distances of a few hundred pc, the photometric distances underestimate the true distances by 60–80% on average. It is important to note that the uncertainties of the photometric distances are relatively large in part due to the range in possible ages, errors in the SpT- T_{eff} conversion with T_{eff} known to $\pm 100\text{K}$, and unknown stellar metallicities.

5.2. Young Moving Group Memberships

We searched for kinematic matches to 14 reported nearby YMGs listed in Table 4. In addition to common *UVW*s, we require that the age of the YMG lie within the age range provided in SLR09 and that the 3-D position of the candidate member coincide in the sky (R.A., Dec., and distance) near the previously reported members (Figure 6) to propose membership to a group. Note that this procedure will favor membership in moving groups spread over the sky (e.g. β Pic and AB Dor).

Given our cutoff criteria of $\Delta v < 8 \text{ km s}^{-1}$, we identify the kinematic matches in Table 5, each with an appended quality flag. This flag scores 3 characteristics with an ‘A’ or ‘B’. These are:

(1) Kinematic matches: ‘A’ for having a trigonometric distance with $\Delta v < 5 \text{ km s}^{-1}$ and $\tilde{\chi}^2 < 6$, a regime where 90% of previously reported YMG members lie (Figure 4), or ‘B’ if the target has only a photometric distance or velocity modulus $\geq 5 \text{ km s}^{-1}$ but $< 8 \text{ km s}^{-1}$ and $\tilde{\chi}^2 \geq 6$ but < 9 . For those stars with this ‘A’ flag, we provide a kinematic membership probability in Table 5 computed by assuming that the $\tilde{\chi}^2$ follows a typical χ^2 distribution with 3 degrees of freedom. The probabilities of the previously-reported members are all $> 10\%$.

(2) Three-dimensional spatial agreement with the YMG: ‘A’ for lying within the 3-D bounds of the YMG, determined by drawing an R.A./Dec. box around all previously-reported members (Figure 6) and falling within the distance range they span (Table 4); and ‘B’ for not. For the loose associations, such as AB Dor, β Pic and UMa, there are no R.A. and Dec. constraints applied but distance agreement is still necessary.

(3) Age agreement with the spectroscopically determined ages: ‘A’ if the YMG’s age falls within the range reported by SLR09 or ‘B’ if it does not.

We consider stars flagged with ‘AAA’ as good YMG members.

Of the 83 M dwarfs with trigonometric distances, 36 stars have kinematics consistent with one of the known YMGs, i.e. kinematic flag = ‘A’. In 13 cases, a star shares its *UVW* with more than one YMG. For these, we disentangled the classification using the star’s sky position and/or spectroscopic age limits. In the end, we identified 21 ‘AAA’ members, 10 of which had been previously reported, plus 17 ‘BAA’ YMG candidates. The Δv and $\tilde{\chi}^2$ distributions of the ‘AAA’ YMG members are very similar to that of the known YMGs with published parallaxes (Figure 4). One might expect then that those stars flagged as ‘ABB’, ‘ABA’, or ‘AAB’, which match YMG kinematics within our velocity in $\tilde{\chi}^2$ limits might have

a different $\tilde{\chi}^2$ distribution, skewed more towards higher values. However, at least for the 15 stars in this category, this is not the case.

By analyzing the kinematics of the stars with parallaxes, we find that there is on average a 4% chance of any given star to appear as a kinematic match (flag = ‘A’) to any one of the 14 YMGs (Figures 7 – 8), with a total of 46 out of a possible 1162 matches (including multiple matches for a given star; Figure 9). Of these 46 matches, 21 are flagged as ‘AAA’ and are very probable YMG members. This leaves us with 54% of the matches which do not adhere to our other two criteria. Due to this high rate of false positives of a Galactic disk star with UVW s matching a YMG within our confidence level, it is critical that common kinematics be only one of several criteria required for group membership.

An example of such a pitfall is the proposed Hyades Stream defined by ~ 30 stars with UVW velocities matching those of the Hyades Cluster (Famaey et al. 2005). Using chemical analysis, de Silva et al. (2011) showed that the metallicity distribution of the stars in the Hyades Stream resembles that of the Galactic field stars rather than of the cluster itself, with only 4 stars matching that of the cluster. Similarly, Famaey et al. (2007) observed the stream stars to have a mass distribution closer to the field than to the Hyades Cluster itself, which is depleted in low-mass stars. Pompéia et al. (2011) interpreted the Hyades Stream as an inner 4:1 resonance of the Galactic spiral pattern, rather than stripped off members of the cluster.

Similarly, Famaey et al. (2008) and Bovy & Hogg (2010) found that the bulk of proposed members of the Pleiades Moving Group, as determined from common UVW s, were not stripped off members of the Pleiades cluster as previously believed. These results demonstrate a valuable lesson. In order to firmly identify YMG members, a confluence of evidence is required, namely, common 3-dimensional space velocities, coherent sky position, consistent age estimates, and when practical (i.e. for FGK stars), compositional homogeneity.

To summarize our findings, we identify with reasonable confidence 9 new members of the AB Dor YMG (50–100 Myr) and 2 members of the Ursa Majoris group (300 Myr), bringing the count up to 43 and 30 members, respectively. We also recovered 10 previously reported YMG members. And with lower probability, we identify 6 possibly new members of the Castor group, 4 of the Ursa Major moving group, 2 AB Dor members, and 1 member each of the Her-Lyr and β Pic groups. We also identify the first 3 members of a potentially new YMG consisting of a binary pair of M dwarfs (2MASS J04465175-1116476 A and B) and a co-moving third M dwarf (GJ 4044). (See Section 7.) Although they are far apart on the sky, they each have a distance of 18 pc and agree in age, both ranging from 40 – 300 Myr.

5.3. Where are all the ‘Missing’ M Dwarf Members?

As noted in Section 1, we expect there to be many more M dwarf members of YMGs than currently known. Although we report a total of 25 new low-mass candidate members (with varying probabilities) of several YMGs, this is only a small fraction of the expected true population. For example, we expect AB Dor to have an additional ≈ 90 M dwarfs yet we found only 1/10 of that (Figure 10).

There are several reasons for this, the most obvious one being the selection criteria of our original SLR09 sample. We selected only targets with declinations greater than -35° , i.e. those accessible to the Mauna Kea telescopes. This eliminated the potential of finding new members of the very southern associations such as η Cha. Yet we still searched for common space-motion objects to these southern YMGs in case of any associated streams of stars. Another factor is *ROSAT*’s insensitivity to finding mid- to late- M dwarfs past 30 pc. According to Figure 11, showing the *ROSAT*-selected sample of Riaz et al. (2006), we would not be sensitive to many young stars later than M4.5. In addition, it may be that the intrinsic dispersion in L_X/L_{Bol} leads us to choose only the most active members of each YMG.

It is also possible that the published FGK members of the YMGs are not all actually members thereby skewing our expected M dwarf count. Lastly, it may even be possible that the mass function of these YMGs strongly differs from the field population, and the M dwarf members are not actually there to be found, as appears to be the case for Taurus star-forming region where the relative number of low-mass stars appears to be deficient compared to other young clusters (Luhman 2004). In order to test the implications of *ROSAT*’s limitations as well as to search for more low-mass YMG members, we are completing a far more sensitive survey of young M dwarfs with photometric distances out to 100 pc using the *GALEX* archive (Shkolnik et al. 2011) and telescopes located in both the northern and southern hemispheres.

6. Visual Binaries

Visual inspection of the images taken during the first epoch of each target revealed 10 VBs, 3 of which were previously unreported. For 8 of these, we use the “lucky imaging” technique (e.g. Law et al. 2006) to measure their separation, position angle and approximate flux ratio in the CAPSCam bandpass. (For the remaining two, 1RXS 2043 and G273-191, the lucky imaging procedure fails as the two components are of near-equal flux.) CAPSCam allows for fast readout of a small window on the detector while integrating deeply on the full field. For standard astrometric observations, this guide window is directly added to

the full field image so the perturbations of the atmosphere and tracking are the same for the target star and the background reference sources. However, since these sub-images are stored in independent files, they can be shifted and added to produce a higher contrast image. This reduction process significantly enhances the contrast of the image resulting in better resolution than that typically allowed by the seeing.

When a close binary was identified, we ran this lucky imaging technique on the sub-images obtained on the first epoch of observation. Between 300 and 1500 sub-images are used to produce the final image. The results for the 10 VBs are shown in Figures 12 and 13. The angular separation, position angle and flux ratio of each pair are computed from the images and are summarized in Table 6. We also searched each field for wide common-proper motion stars to our targets and found 4 such systems, which are described in more detail below.

In addition to these relatively wide visual binaries, many stars in the SLR09 sample have been resolved into very tight binary systems through a separate high contrast adaptive optics (AO) imaging program being carried out at the Keck and Subaru telescopes (Bowler et al. (2012), in press, and in preparation). These binaries resolved with AO are identified with a “(AB)” designation in the tables and are not resolved in our CAPSCam data. The natural guide star AO observations were conducted with the Near Infrared Camera 2 (NIRC2) in its narrow field mode on Keck-II and the High Contrast Instrument for the Subaru Next Generation Adaptive Optics (HiCIAO; Hodapp et al. 2008) imager on Subaru. Table 7 lists the flux ratios of the resolved binaries, which were derived by fitting analytical models made of the sum of three elliptical Gaussians for each binary component as described in Liu et al. (2008). The quoted values and uncertainties are the mean and standard deviations from fits to individual images. We found that variations in the input model (e.g., two versus three Gaussians per binary component) resulted in systematic errors in the resulting flux ratios of $\sim 5\%$ for blended binaries and $\sim 1\%$ for well separated systems. We therefore add 5% and 1% of the flux ratios in quadrature with the random errors we measure for binaries with separations < 150 mas and > 150 mas, respectively. More details about our observations will appear in an upcoming paper describing this AO imaging survey.

7. Notes on Individual Targets

2MASS J00034227–2822410 is an M7 dwarf common proper motion companion to the G8.5V star HD 225118 lying $65.35''$ away, first noticed by Cruz et al. (2007). We confirmed this companionship with mutually consistent RVs: $RV_{G8} = 10.6 \pm 0.3 \text{ km s}^{-1}$ (Crifo et al. 2010) and $RV_{M7} = 11.6 \pm 1.1 \text{ km s}^{-1}$. Using CAPSCam, we measured the distance to the G8

star to be 36.1 ± 3.9 pc, in good agreement with distance to the M7 dwarf of 38.6 ± 4.0 pc measured by Dupuy & Liu (2012, in press).⁴ Faherty et al. (2010)⁵ determined that the age of the M dwarf is between 0.1 and 1 Gyr because it does not display signs of low gravity yet is still X-ray active (West et al. 2008). Similarly, SLR09 find no indication of low gravity in its optical spectrum. Its strong X-ray activity implies a probable upper age limit of ~ 300 Myr. However, Faherty et al. (2010) provide an age range for the primary of 0.9 to 1.4 Gyr based on Ca II activity age (Mamajek & Hillenbrand 2008). Given this inconsistency, the age of the system could be between 0.3 and 1 Gyr.

G 132-51 B (E & W) is a common proper-motion companion to G 132-50 AB (see Table 7). Including G 132-51 A makes this a quintuple system in the AB Dor Moving Group.

G 271-110 has recently been identified as a common-proper motion companion to EX Cet by Alonso-Floriano et al. (2011), a known young star reported to be part of the Local Association by Montes et al. (2001). We measure the RV of G 271-110 to be 12.2 ± 0.4 km s⁻¹ which is consistent with the published RV of EX Cet (11.6 ± 0.6 km s⁻¹, Montes et al. 2001). We therefore adopt the Hipparcos distance of 24 pc of EX Cet for G 271-110. We calculate UVW of (-13.2, -19.1, -11.8) km s⁻¹ making it a good kinematic match to the Pleiades, albeit very distant in 3-D space from the cluster.

2MASS J03350208+2342356 is an M8.5 brown dwarf. It has detected lithium absorption and signs of ongoing accretion, setting an upper age limit of 10 Myr. Its UVW velocities produce Δv of 7 km s⁻¹ making it a lower-probability (8%) ‘BAA’ member of the β Pic YMG. If this BD is indeed a member, then it would be equal to the lowest mass member known, 2MASS J06085283-2753583 (Rice et al. 2010), which has a Δv of ~ 4 km s⁻¹.

G 269-153 NE, SW, E = GJ 2022 ABC: RVs for these three AB Dor members agree, and we adopt a trigonometric distance of 12.6 ± 2.3 pc for the system based on our parallax for the brightest component. At the times of our observations, between UT20090909 (Figure 14) and UT20101114, the NE (SpT=M4.3) and SW (SpT=M4.6) components were $< 1''$ apart, closer than the $2.0''$ reported by Daemgen et al. (2007) in both 1999 and 2005. This difference is likely due to the orbital motion of the binary. Since the C component, lying $38''$ eastward, was not included in the original SLR09 sample, we observed it with the MIKE high-resolution optical spectrograph at the Magellan (Clay) Telescope. We measured its RV to be $18.24 \pm$

⁴We were unable to obtain a reliable parallax for the M dwarf due to its faintness.

⁵Note that the UVW s reported for the M dwarf by Faherty et al. (2010) are inconsistent with ours, yet the proper motions, distances and RVs generally agree.

0.45 km s⁻¹ and its SpT as M5.

GJ 3305 AB (SpT = M1.1) is resolved as a tight binary by high-resolution imaging by Delorme et al. (2012) and Bowler et al. (in preparation), but not by us using CAPSCam. It is a clear common proper motion companion to the β Pic YMG member and F0V star 51 Eri (HD 29391) separated by 66.7'' (Feigelson et al. 2006). The RV of 51 Eri is 21.0 ± 1.8 km s⁻¹ (Kharchenko et al. 2007), which agrees with that of GJ 3305 AB (21.7 ± 0.3 km s⁻¹). Thus we use 51 Eri’s Hipparcos distance of 29.8 ± 0.8 pc to calculate the *UVW* for GJ 3305 AB. At this distance, the separation between 51 Eri and GJ 3305 AB is 2200 AU.

NLTT 13728 is a newly confirmed young M6 brown dwarf within 10 pc. We measured its distance to be 9.5 ± 0.3 pc with an upper age limit of 90 Myr based on signatures of low-gravity and strong H α emission (SLR09).

2MASS J04465175–1116476 AB: is a binary pair with a separation of 1.59'' and a position angle of 279°. The primary (east component; SpT=M4.9) is 1.93 times brighter than the secondary (SpT=M6) in the CAPSCam bandpass (roughly I band). The binary and its co-moving companion GJ 4044 have distances of 18.6 ± 1.7 pc and 17.2 ± 0.7 pc, respectively, and *UVW*s of $(-5.3 \pm 0.7, -0.9 \pm 1.2, -20.0 \pm 1.2)$ and $(-4.7 \pm 0.5, 0.3 \pm 0.5, -19.5 \pm 0.8)$ km s⁻¹. Although they are far apart on the sky (separated by 212°), they do agree in age, both ranging from 40 – 300 Myr.

2MASS J05575096–1359503 is a young M7 object with a photometric distance of 60 pc using an age of 10 Myr and the Baraffe et al. (1998) models. However, the parallax is so small that the distance to this object is formally measured to be 526 ± 277 pc. This larger distance implies that the object is a brown dwarf younger than 2 Myr.

NLTT 15049 is another tight VB with the primary (SpT=M3.8) lying SW of the secondary (SpT=M5). The separation is 0.47'' with a position angle of 56° and a CAPSCam flux ratio of ≈ 3 .

CD-35 2722 is an M1 star reported to have a wide substellar companion by Wahhaj et al. (2011). Our kinematic and age analysis identifies this system as a highly-probable (98%) AB Dor member, agreeing well with the results of Wahhaj et al. (2011).

1RXS J101432.0+060649 AB is a new VB with the primary (M4.1) lying east of the secondary (M4.5) with a separation of 2.02'', a position angle of 271°, and a CAPSCam flux ratio of 1.2.

2MASS J10364483+1521394 AB is a triple system where the northern component (A; SpT=M4) is 1.7 times brighter in the CAPSCam bandpass than the southern component (B;

SpT = M4.5+M4.5) with a separation of $0.96''$ and a position angle of 160° . Daemgen et al. (2007) reported a separation of the components of 2MASS J10364483+1521394 B to be $0.189''$, undetectable by us as this separation corresponds to about one CAPSCam pixel.

NLTT 56194 has a SpT of M7.5 and a photometric distance of 14 ± 3 pc with a spectroscopic age of 100–300 Myr. It is a kinematic match, with a quality flag of ‘B’, to the Castor group (200 Myr). This make NLTT 56194 another young BD in our sample.

8. Summary

We present a kinematic analysis of the 165 young ($\lesssim 300$ Myr), nearby and X-ray-bright M dwarfs compiled by SLR09. We have further characterized this “25-pc sample” with radial velocities and distances, showing that nearly half are outside of 25 pc as expected if they are indeed young. We acquired distances for half the sample from trigonometric parallaxes while we estimated photometric distances for the remainder of the sample using models and correcting for visual binarity and youth determined from spectroscopic age indicators. Our astrometric survey showed that for this sample of young stars, photometric distances underestimate the true distances by an average of roughly 70%, and range from 5 to 500 pc. This implies that the *UVW*s of young stars based on photometric distances that assume the stars lie on the main-sequence are most likely unreliable.

By combining our RVs and distances with proper motions, we calculated the targets’ *UVW* velocities in search of new YMG members. We identified 21 likely members of YMGs, which have accurate *UVW*s determined from trigonometric parallaxes, positional coincidence with known members, and age agreement using the independent spectroscopic and X-ray age diagnostics presented in SLR09. Of these, 10 were previously known AB Dor, Hyades, or β Pic members. Newly proposed members include 9 AB Dor members and 2 UMa members. Additional possible candidates include 6 Castor members, 4 Ursa Majoris members, 2 AB Dor members, and 1 member each of the Her-Lyr and β Pic groups.

In addition, we identified three stars (two of which form a binary pair) with identical kinematics and age ranges, potentially forming their own young association. We also found kinematic matches to YMGs for 40 stars, but either their positions on the sky or ages do not agree with previously known members. For 12 stars that are kinematic and age matches but are positionally offset to the other group members, chemical analysis would be one way to confirm that the stars did indeed originate from a common star-forming event. However, metallicity indicators of M dwarfs may not yet be accurate or precise enough to discriminate group members from the field population (e.g. Neves et al. 2011 and references therein).

Lastly, our sample also contains 31 young M dwarfs, including 4 brown dwarfs, with ages $\lesssim 150$ Myr, which are not associated with any known YMG.

Even relaxing the requirements of spectroscopic and positional age agreement, we did not recover the expected numbers of M dwarf members to the YMGs. After accounting for our observing limitations, the likeliest explanation is that the *ROSAT* All-Sky Survey is not sensitive enough to detect YMG members lying beyond 25–30 pc. In order to understand this further, as well as identify even more members, we are completing a larger survey of young M dwarfs with photometric distances out to 100 pc using the more sensitive *GALEX* archive.

We appreciate the spectrum of G 269-153 (E) taken by Julio Chaname and CAPSCam data observed by Stella Kafka. We would like to thank the CFHT, Keck and LCO staff for their care in setting up the instruments and support in the control rooms, and to J.-F. Donati for making *Libre-ESpRIT* available to CFHT users. We would also like to thank the referee, Sébastien Lépine, for a careful review of the manuscript. Funding from the Carnegie Institution of Washington for E.S. and G.A.-E. is gratefully acknowledged. Funding for M.C.L. and B.P.B. has in part been provided by NSF grant AST09-09222 and NASA grant NNX11AC31G. We also acknowledge partial support for the LCO observing by the NASA Astrobiology Institute under cooperative agreement NNA09DA81A. This publication makes use of data products from the Two Micron All Sky Survey, which is a joint project of the University of Massachusetts and the Infrared Processing and Analysis Center/California Institute of Technology, funded by the National Aeronautics and Space Administration and the National Science Foundation.

REFERENCES

- Alonso-Floriano, F. J., Caballero, J. A., & Montes, D. 2011, in *Stellar Clusters & Associations: A RIA Workshop on Gaia*, 344–347
- Anglada-Escudé, G., Boss, A. P., Weinberger, A. J., Thompson, I. B., Butler, R. P., Vogt, S. S., & Rivera, E. J. 2011, *ArXiv e-prints*
- Baraffe, I., Chabrier, G., Allard, F., & Hauschildt, P. H. 1998, *A&A*, 337, 403
- Baraffe, I., Chabrier, G., Barman, T. S., Allard, F., & Hauschildt, P. H. 2003, *A&A*, 402, 701
- Barrado y Navascués, D., Stauffer, J. R., & Patten, B. M. 1999, *ApJ*, 522, L53
- Bochanski, J. J., Hawley, S. L., Covey, K. R., West, A. A., Reid, I. N., Golimowski, D. A., & Ivezić, Ž. 2010, *AJ*, 139, 2679
- Boss, A. P. 2011, *ApJ*, 731, 74
- Boss, A. P., et al. 2009, *PASP*, 121, 1218
- Bovy, J., & Hogg, D. W. 2010, *ApJ*, 717, 617
- Bowler, B. P., Liu, M. C., Shkolnik, E. L., Dupuy, T. J., Cieza, L. A., Kraus, A. L., & Tamura, M. 2012, *ArXiv e-prints*
- Burrows, A., et al. 1997, *ApJ*, 491, 856
- Crifo, F., Jasniewicz, G., Soubiran, C., Katz, D., Siebert, A., Veltz, L., & Udry, S. 2010, *A&A*, 524, A10+
- Crockett, C. J., Mahmud, N. I., Prato, L., Johns-Krull, C. M., Jaffe, D. T., & Beichman, C. A. 2011, *ApJ*, 735, 78
- Cruz, K. L., et al. 2007, *AJ*, 133, 439
- Cruz, K. L., Reid, I. N., Liebert, J., Kirkpatrick, J. D., & Lowrance, P. J. 2003, *AJ*, 126, 2421
- Daemgen, S., Siegler, N., Reid, I. N., & Close, L. M. 2007, *ApJ*, 654, 558
- de Silva, G. M., Freeman, K. C., Bland-Hawthorn, J., Asplund, M., Williams, M., & Holmberg, J. 2011, *MNRAS*, 415, 563

- Delorme, P., Lagrange, A. M., Chauvin, G., Bonavita, M., Lacour, S., Bonnefoy, M., Ehrenreich, D., & Beust, H. 2012, *A&A*, 539, A72
- Faherty, J. K., Burgasser, A. J., West, A. A., Bochanski, J. J., Cruz, K. L., Shara, M. M., & Walter, F. M. 2010, *AJ*, 139, 176
- Famaey, B., Jorissen, A., Luri, X., Mayor, M., Udry, S., Dejonghe, H., & Turon, C. 2005, *A&A*, 430, 165
- Famaey, B., Pont, F., Luri, X., Udry, S., Mayor, M., & Jorissen, A. 2007, *A&A*, 461, 957
- Famaey, B., Siebert, A., & Jorissen, A. 2008, *A&A*, 483, 453
- Feigelson, E. D., Lawson, W. A., Stark, M., Townsley, L., & Garmire, G. P. 2006, *AJ*, 131, 1730
- Gizis, J. E., Reid, I. N., & Hawley, S. L. 2002, *AJ*, 123, 3356
- Hernán-Obispo, M., Gálvez-Ortiz, M. C., Anglada-Escudé, G., Kane, S. R., Barnes, J. R., de Castro, E., & Cornide, M. 2010, *A&A*, 512, A45
- Hillenbrand, L. A., et al. 2008, *ApJ*, 677, 630
- Hodapp, K. W., et al. 2008, in *Society of Photo-Optical Instrumentation Engineers (SPIE) Conference Series*, Vol. 7014, Society of Photo-Optical Instrumentation Engineers (SPIE) Conference Series
- Høg, E., et al. 2000, *A&A*, 355, L27
- Jameson, R. F., Casewell, S. L., Bannister, N. P., Lodieu, N., Keresztes, K., Dobbie, P. D., & Hodgkin, S. T. 2008, *MNRAS*, 384, 1399
- Jeffries, R. D. 1995, *MNRAS*, 273, 559
- Johnson, D. R. H., & Soderblom, D. R. 1987, *AJ*, 93, 864
- Kasper, M., Apai, D., Janson, M., & Brandner, W. 2007, *A&A*, 472, 321
- Kharchenko, N., Kilpio, E., Malkov, O., & Schilbach, E. 2002, *A&A*, 384, 925
- Kharchenko, N. V., Scholz, R.-D., Piskunov, A. E., Röser, S., & Schilbach, E. 2007, *Astronomische Nachrichten*, 328, 889
- King, J. R., & Schuler, S. C. 2005, *PASP*, 117, 911

- Kraus, A. L., & Ireland, M. J. 2011, ArXiv e-prints
- Lagrange, A.-M., et al. 2010, *Science*, 329, 57
- Law, N. M., Mackay, C. D., & Baldwin, J. E. 2006, *A&A*, 446, 739
- Leggett, S. K., Allard, F., Dahn, C., Hauschildt, P. H., Kerr, T. H., & Rayner, J. 2000, *ApJ*, 535, 965
- Leggett, S. K., Allard, F., Geballe, T. R., Hauschildt, P. H., & Schweitzer, A. 2001, *ApJ*, 548, 908
- Lépine, S., & Shara, M. M. 2005, *AJ*, 129, 1483
- Lépine, S., & Simon, M. 2009, *AJ*, 137, 3632
- Liu, M. C., Dupuy, T. J., & Ireland, M. J. 2008, *ApJ*, 689, 436
- Liu, M. C., et al. 2010, in *Society of Photo-Optical Instrumentation Engineers (SPIE) Conference Series*, Vol. 7736, Society of Photo-Optical Instrumentation Engineers (SPIE) Conference Series
- López-Santiago, J., Montes, D., Crespo-Chacón, I., & Fernández-Figueroa, M. J. 2006, *ApJ*, 643, 1160
- López-Santiago, J., Montes, D., Gálvez-Ortiz, M. C., Crespo-Chacón, I., Martínez-Arnáiz, R. M., Fernández-Figueroa, M. J., de Castro, E., & Cornide, M. 2010, *A&A*, 514, A97+
- Luhman, K. L. 2004, *ApJ*, 617, 1216
- Mamajek, E. E., & Hillenbrand, L. A. 2008, *ApJ*, 687, 1264
- Marois, C., Macintosh, B., Barman, T., Zuckerman, B., Song, I., Patience, J., Lafrenière, D., & Doyon, R. 2008, *Science*, 322, 1348
- McCarthy, C., Zuckerman, B., & Becklin, E. E. 2001, *AJ*, 121, 3259
- Mentuch, E., Brandeker, A., van Kerkwijk, M. H., Jayawardhana, R., & Hauschildt, P. H. 2008, *ApJ*, 689, 1127
- Mochmacki, S. W., et al. 2002, *AJ*, 124, 2868
- Monet, D. G., et al. 2003, *AJ*, 125, 984

- Montes, D., López-Santiago, J., Gálvez, M. C., Fernández-Figueroa, M. J., De Castro, E., & Cornide, M. 2001, *MNRAS*, 328, 45
- Neves, V., et al. 2011, ArXiv e-prints
- Perryman, M. A. C., & ESA, eds. 1997, ESA Special Publication, Vol. 1200, The HIPPARCOS and TYCHO catalogues. Astrometric and photometric star catalogues derived from the ESA HIPPARCOS Space Astrometry Mission
- Pompéia, L., et al. 2011, *MNRAS*, 415, 1138
- Prato, L., Huerta, M., Johns-Krull, C. M., Mahmud, N., Jaffe, D. T., & Hartigan, P. 2008, *ApJ*, 687, L103
- Preibisch, T., & Feigelson, E. D. 2005, *ApJS*, 160, 390
- Reid, I. N., & Cruz, K. L. 2002, *AJ*, 123, 2806
- Reid, I. N., et al. 2003, *AJ*, 126, 3007
- . 2004, *AJ*, 128, 463
- Reid, I. N., Cruz, K. L., & Allen, P. R. 2007a, *AJ*, 133, 2825
- Reid, I. N., Cruz, K. L., Kirkpatrick, J. D., Allen, P. R., Mungall, F., Liebert, J., Lowrance, P., & Sweet, A. 2008, *AJ*, 136, 1290
- Reid, I. N., Hawley, S. L., & Gizis, J. E. 1995, *AJ*, 110, 1838
- Reid, I. N., Turner, E. L., Turnbull, M. C., Mountain, M., & Valenti, J. A. 2007b, *ApJ*, 665, 767
- Riaz, B., Gizis, J. E., & Harvin, J. 2006, *AJ*, 132, 866
- Rice, E. L., Faherty, J. K., & Cruz, K. L. 2010, *ApJ*, 715, L165
- Rieke, G. H., et al. 2005, *ApJ*, 620, 1010
- Rodríguez, D. R., Bessell, M. S., Zuckerman, B., & Kastner, J. H. 2011, *ApJ*, 727, 62
- Röser, S., Schilbach, E., Piskunov, A. E., Kharchenko, N. V., & Scholz, R.-D. 2011, *A&A*, 531, A92+
- Salim, S., & Gould, A. 2003, *ApJ*, 582, 1011

- Schlieder, J. E., Lépine, S., & Simon, M. 2010, *AJ*, 140, 119
- . 2012, ArXiv e-prints
- Shkolnik, E., Liu, M. C., & Reid, I. N. 2009, *ApJ*, 699, 649
- Shkolnik, E. L., Hebb, L., Liu, M. C., Reid, I. N., & Cameron, A. C. 2010, *ApJ*, 716, 1522
- Shkolnik, E. L., Liu, M. C., Reid, I. N., Dupuy, T., & Weinberger, A. J. 2011, *ApJ*, 727, 6
- Soderblom, D. R. 2010, *ARA&A*, 48, 581
- Stauffer, J. R., Schultz, G., & Kirkpatrick, J. D. 1998, *ApJ*, 499, L199+
- Stern, R. A., Schmitt, J. H. M. M., & Kahabka, P. T. 1995, *ApJ*, 448, 683
- Torres, C. A. O., Quast, G. R., da Silva, L., de La Reza, R., Melo, C. H. F., & Sterzik, M. 2006, *A&A*, 460, 695
- Torres, C. A. O., Quast, G. R., Melo, C. H. F., & Sterzik, M. F. 2008, *Young Nearby Loose Associations (Handbook of Star Forming Regions, Volume II: The Southern Sky ASP Monograph Publications, Vol. 5. Edited by Bo Reipurth, p.757)*, 757–+
- van Altena, W. F., Lee, J. T., & Hoffleit, E. D. 1995, *The general catalogue of trigonometric [stellar] parallaxes*, ed. van Altena, W. F., Lee, J. T., & Hoffleit, E. D.
- Voges, W., et al. 1999, *A&A*, 349, 389
- . 2000, *VizieR Online Data Catalog*, 9029, 0
- Wahhaj, Z., et al. 2011, *ApJ*, 729, 139
- Webb, R. A., Zuckerman, B., Platais, I., Patience, J., White, R. J., Schwartz, M. J., & McCarthy, C. 1999, *ApJ*, 512, L63
- West, A. A., Hawley, S. L., Bochanski, J. J., Covey, K. R., Reid, I. N., Dhital, S., Hilton, E. J., & Masuda, M. 2008, *AJ*, 135, 785
- White, R. J., Gabor, J. M., & Hillenbrand, L. A. 2007, *AJ*, 133, 2524
- Yee, J. C., & Jensen, E. L. N. 2010, *ApJ*, 711, 303
- Zacharias, N., Monet, D. G., Levine, S. E., Urban, S. E., Gaume, R., & Wycoff, G. L. 2005, *VizieR Online Data Catalog*, 1297, 0

Zacharias, N., Urban, S. E., Zacharias, M. I., Wycoff, G. L., Hall, D. M., Monet, D. G., & Rafferty, T. J. 2004, *AJ*, 127, 3043

Zuckerman, B., Rhee, J. H., Song, I., & Bessell, M. S. 2011, *ApJ*, 732, 61

Zuckerman, B., & Song, I. 2004, *ARA&A*, 42, 685

Zuckerman, B., Song, I., & Bessell, M. S. 2004, *ApJ*, 613, L65

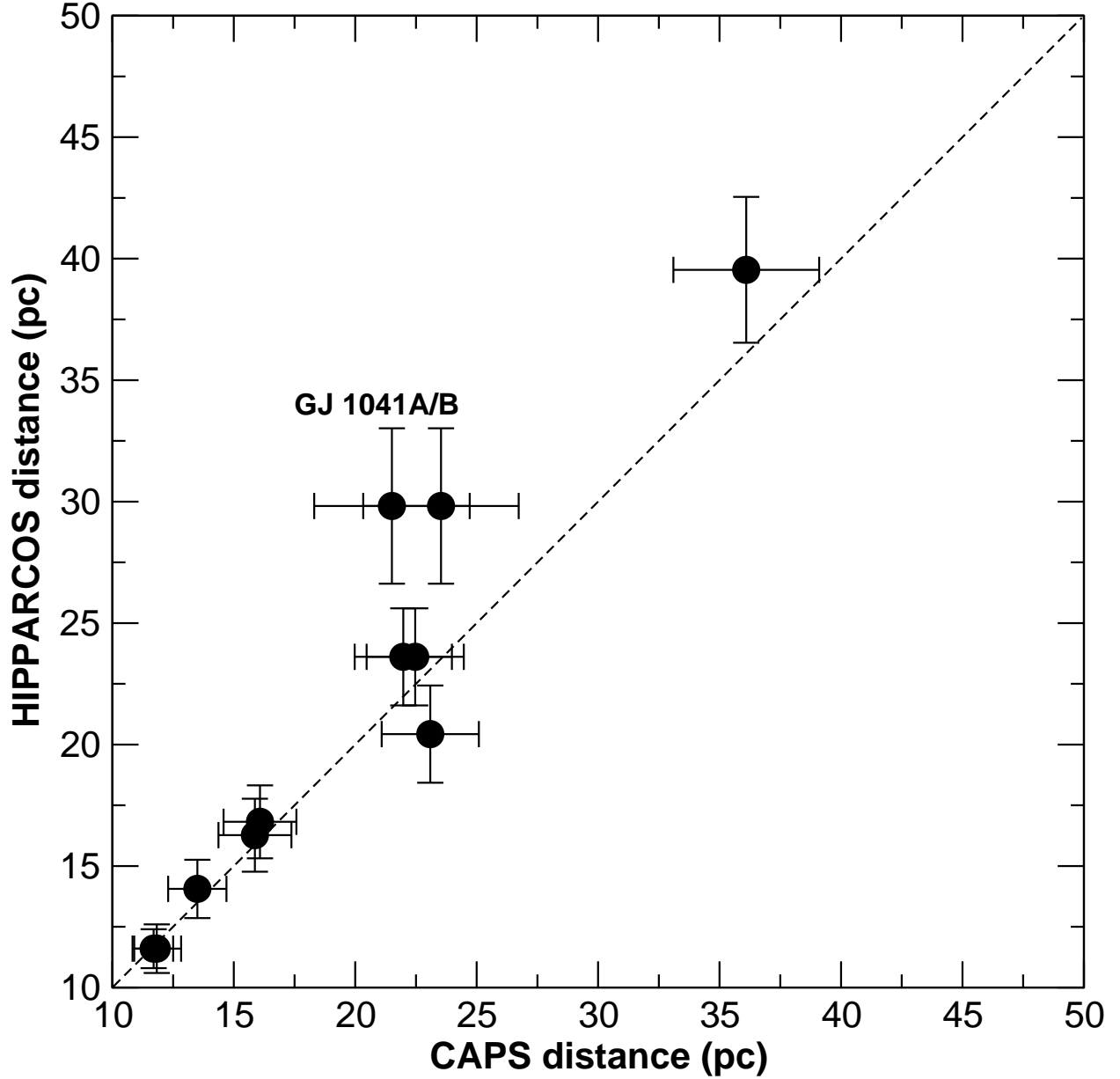


Fig. 1.— A comparison of our trigonometric distances to stars with existing Hipparcos distances. The agreement is consistent within the expected uncertainties except for GJ 1041AB. This is a 4'' binary with components of similar brightness, so both the Hipparcos and CAPSCam parallaxes might be affected by centroid systematics. Excluding GJ 1041 AB, the RMS of the differences is 1.6 pc or 10% relative error with a $\tilde{\chi}^2$ of 0.888 (with 8 degrees of freedom). The data are listed in Table 3.

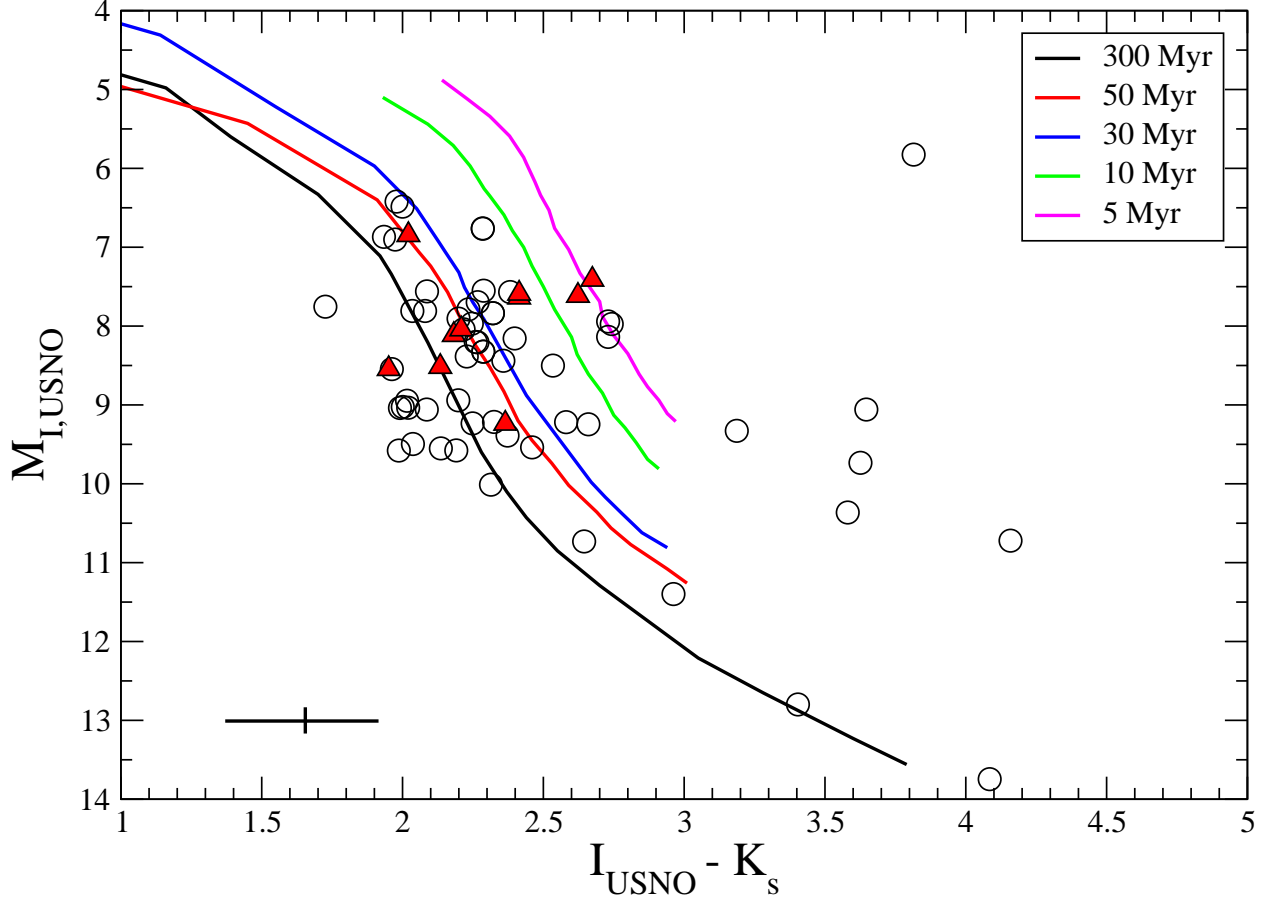


Fig. 2.— A color-magnitude diagram of the targets with parallaxes compared to Baraffe et al. (1998) isochrones. The proposed YMG members with a ‘AAA’ quality flag are marked as triangles. Note that stars with missing or unreliable USNO and/or 2MASS photometry are not included.

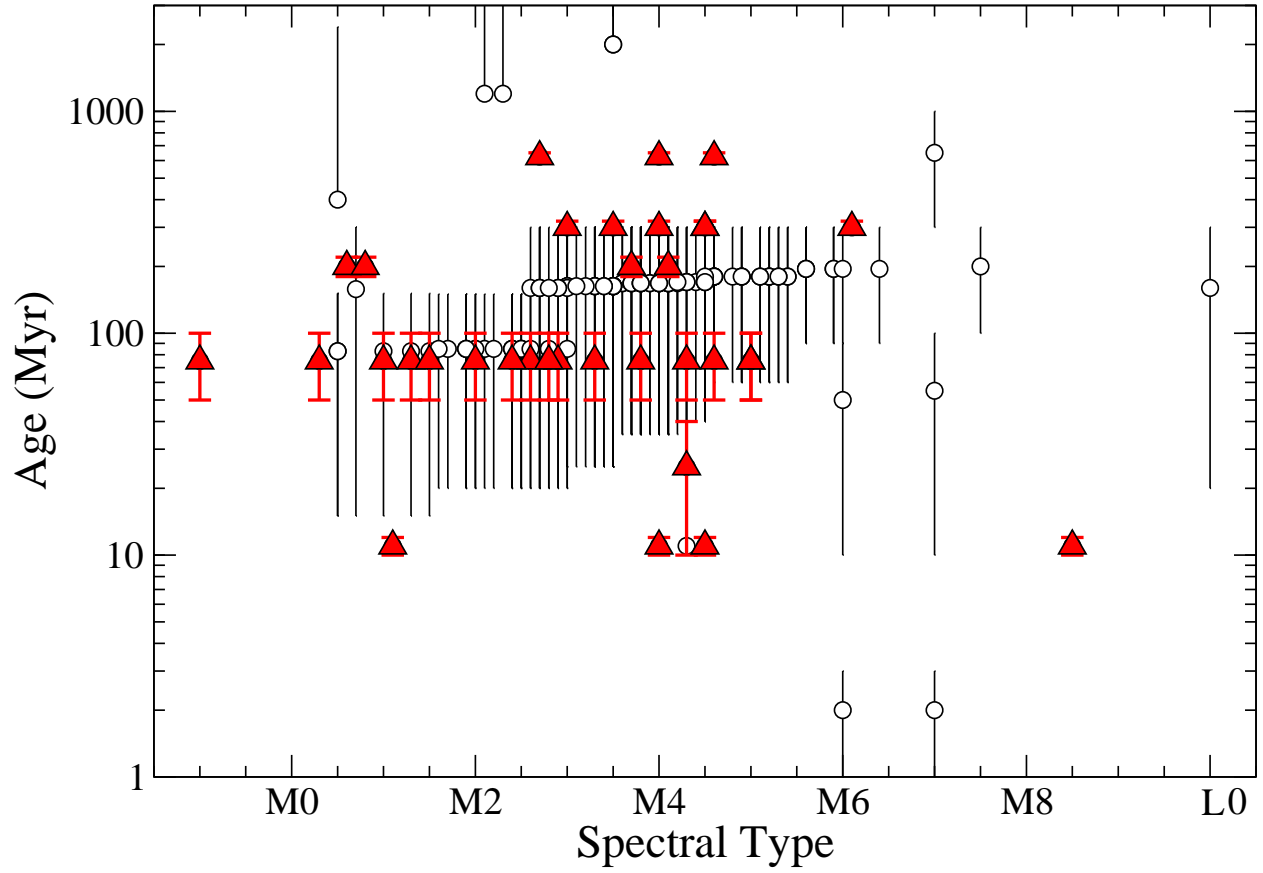


Fig. 3.— Age distribution of our sample. The red triangles are YMG members for which the ages are more precise than those with age limits determined from the spectroscopic indicators alone.

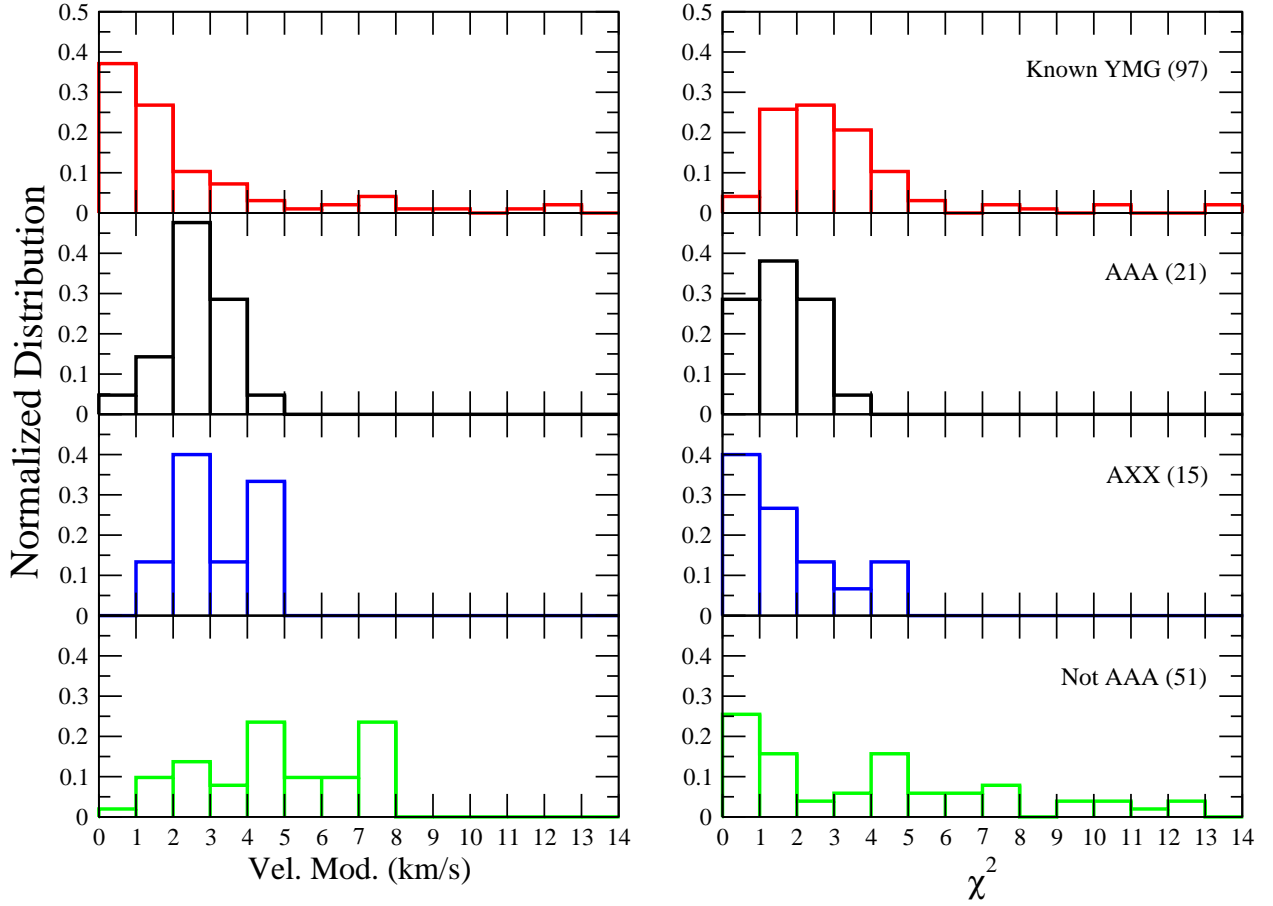


Fig. 4.— The velocity modulus and $\tilde{\chi}^2$ distribution of the known YMG members (AB Dor, TucHor, and β Pic) from Zuckerman & Song (2004) with published parallaxes. Interestingly, the ABB, ABA, and AAB members (see Section 5.2) also have a comparable $\tilde{\chi}^2$ distribution. We define a good kinematic match as having velocity moduli $< 5 \text{ km s}^{-1}$ and $\tilde{\chi}^2 < 6$ with possible matches having $\Delta v < 8 \text{ km s}^{-1}$ and $\tilde{\chi}^2 < 9$.

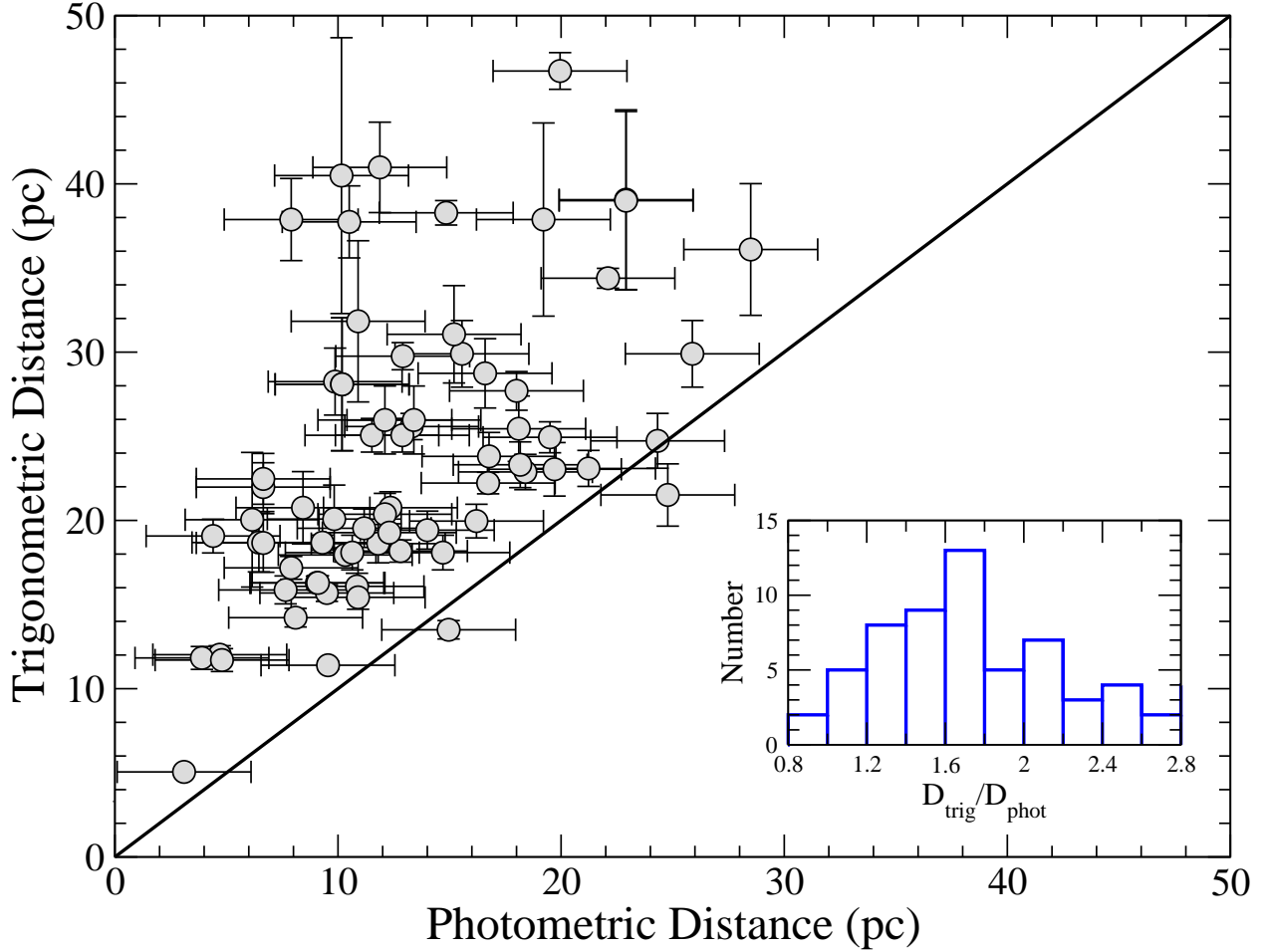


Fig. 5.— Comparison between photometric and trigonometric distances. The photometric distances have been corrected for their youth using upper age limits and known binarity. Note, two points are excluded for the youngest stars (2MASS J0557–1359 and 2MASS J1553–2049) which have distances $\gtrsim 300$ pc.

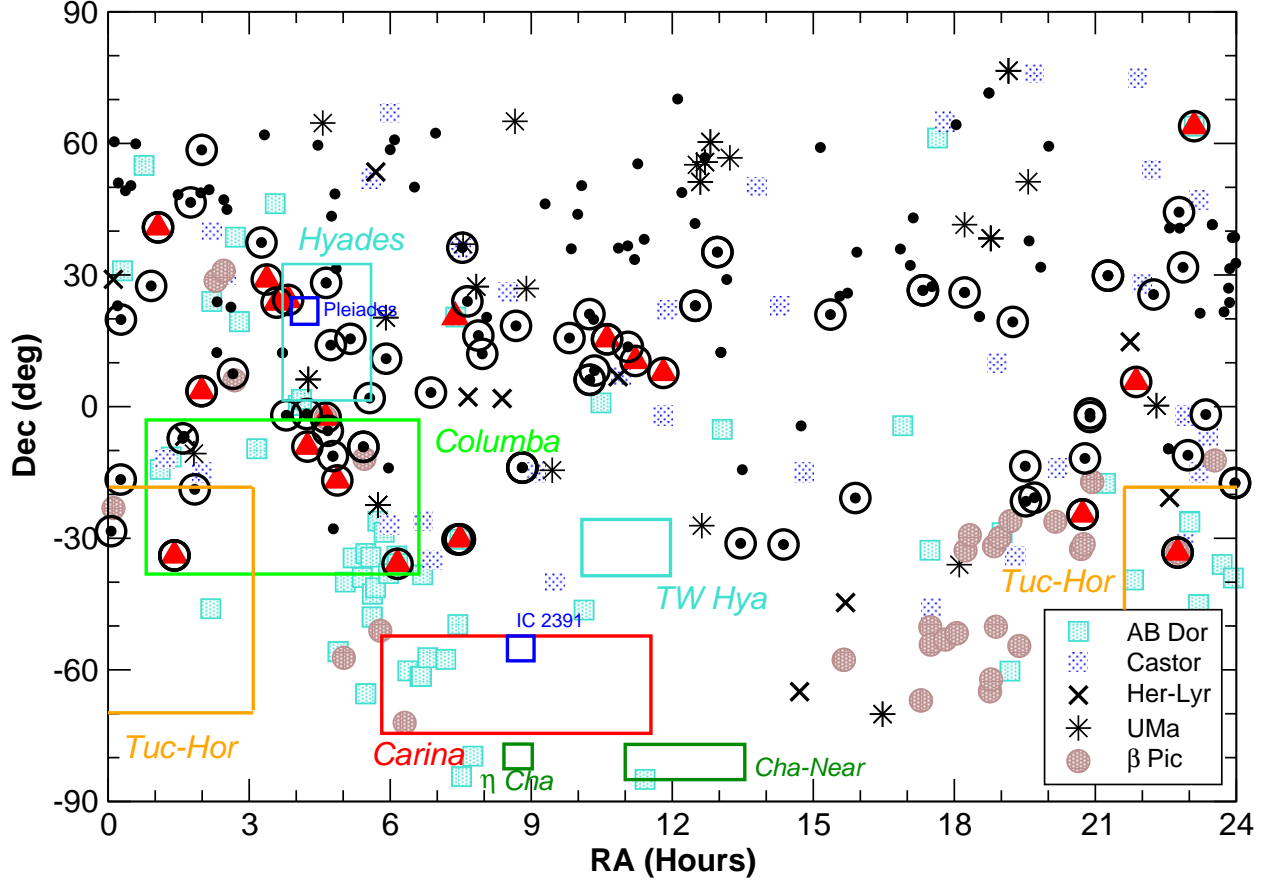


Fig. 6.— Whole sky representation of our targets (black dots) and the YMGs. Those with parallaxes are marked with black circles. The stars with a high-likelihood of membership to a YMG (i.e. ‘AAA’ designation in Table 5) are marked with red triangles. The sources for the known members are: Montes et al. (2001); Zuckerman & Song (2004); López-Santiago et al. (2006, 2010); Torres et al. (2008).

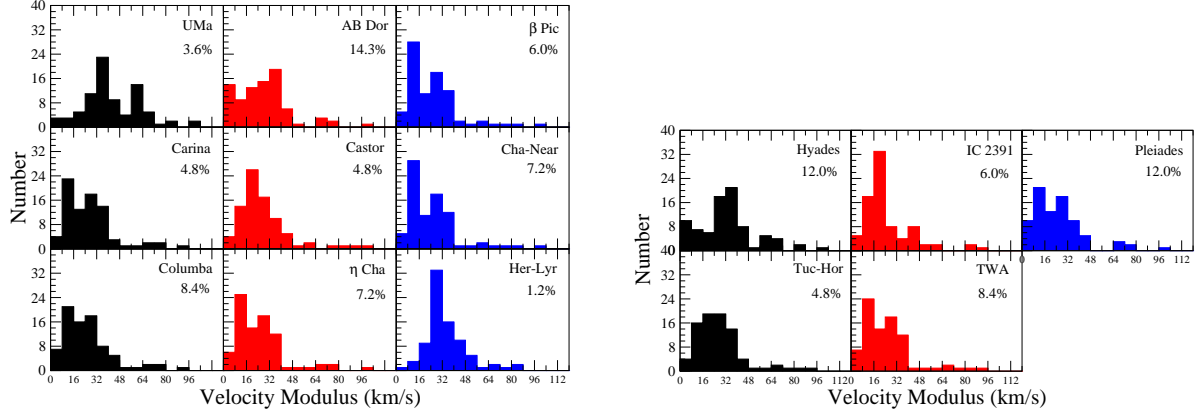


Fig. 7.— Velocity modulus distribution of the 83 targets with parallaxes as measured for each of the 14 YMGs. The percentages listed for each YMG represents the number of kinematic matches found to that group, i.e. the fraction of targets found in the first bin (<8 km/s).

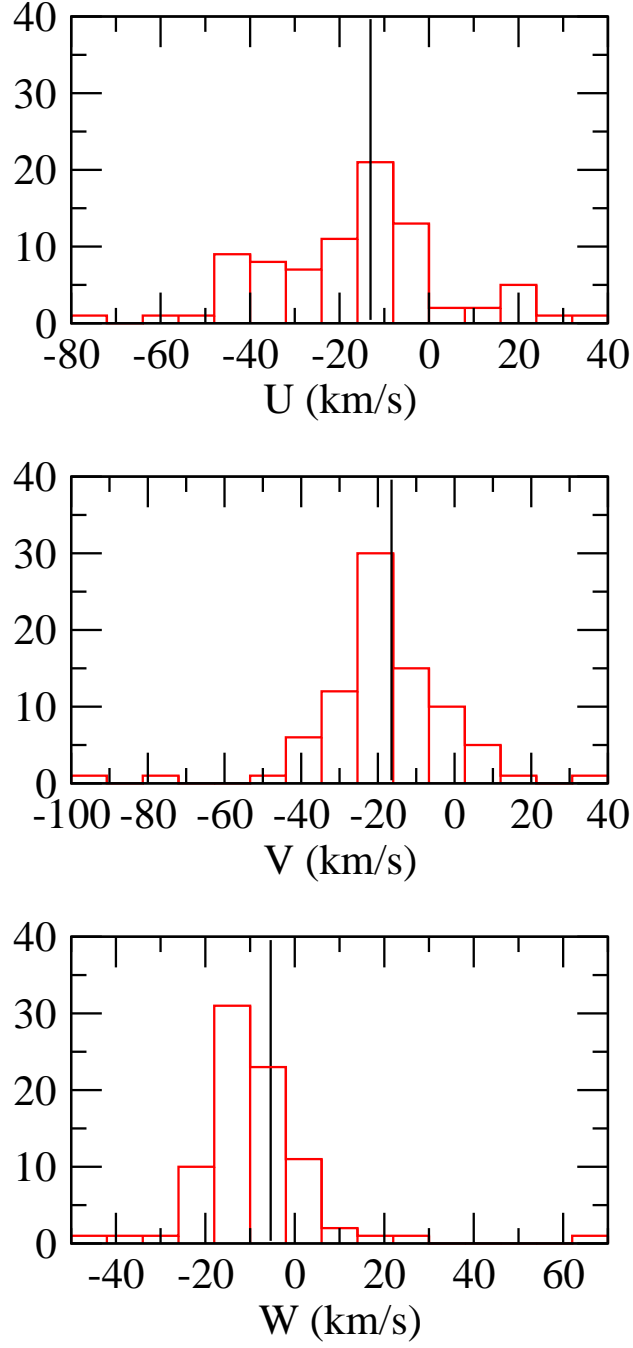


Fig. 8.— UVW distribution of the 83 targets with parallaxes. The solid line represents the mean U , V and W of the YMGs.

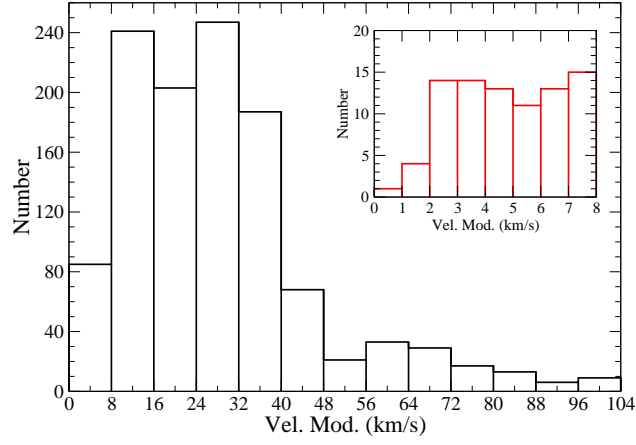


Fig. 9.— Combined velocity modulus distribution for the stars with parallaxes as measured for all the YMG. Eighty-six kinematic matches (with $\Delta v < 8 \text{ km s}^{-1}$) were found out of a possible 1162 ($=83 \text{ targets} \times 14 \text{ YMGs}$) matches. A cut of 5 km s^{-1} produces 46 matches.

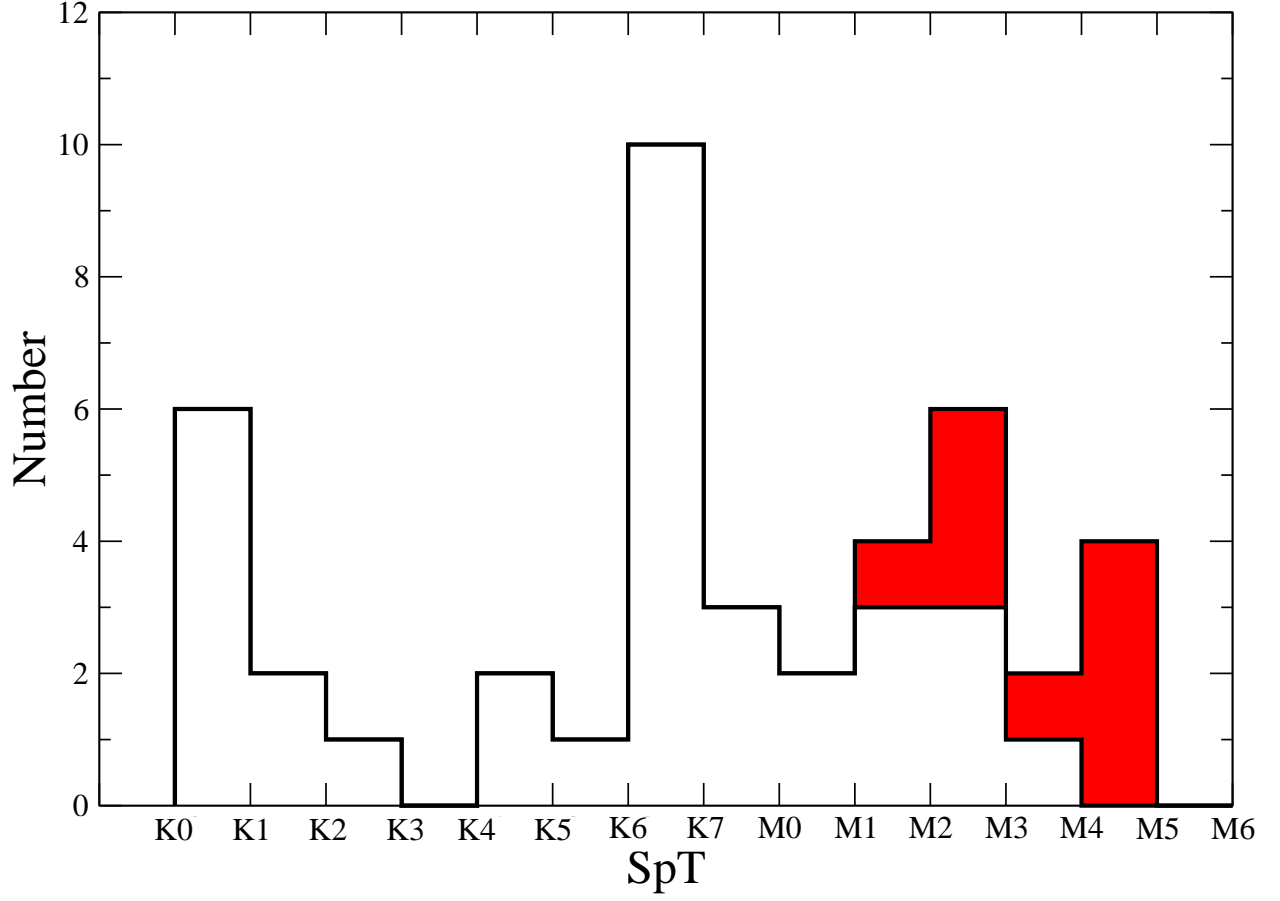


Fig. 10.— SpT histogram of previously reported AB Dor members (black; Zuckerman et al. 2004, 2011; Schlieder et al. 2010) with our 9 proposed AB Dor members (red). The bins represent the number of stars in each spectral type range, e.g., the last bin contains those stars with SpTs $>M4$ and $\leq M5$.

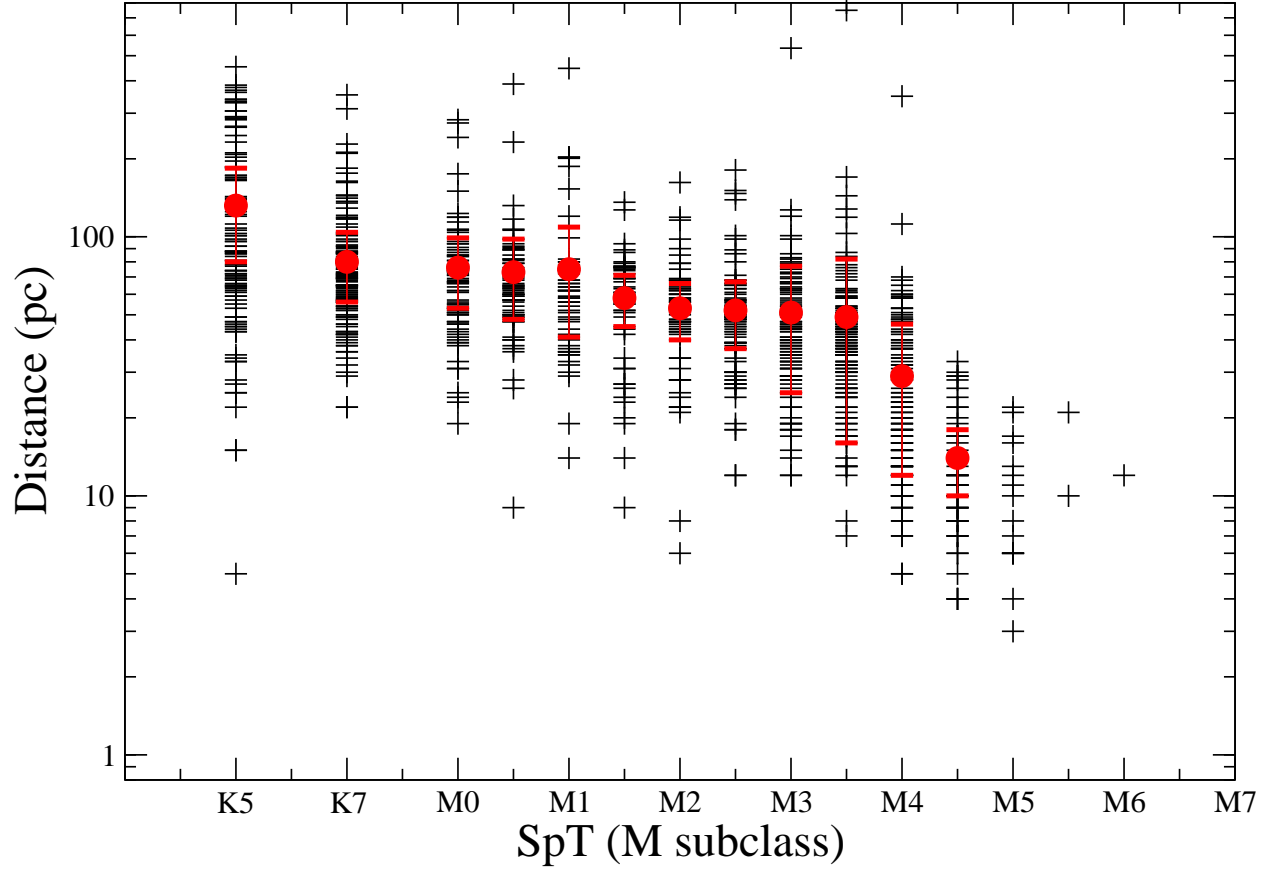


Fig. 11.— The SpT and photometric distance distribution of the Riaz et al. (2006) sample of *ROSAT* selected late-K and M stars. Red points are the mean values with 1 standard deviation bars.

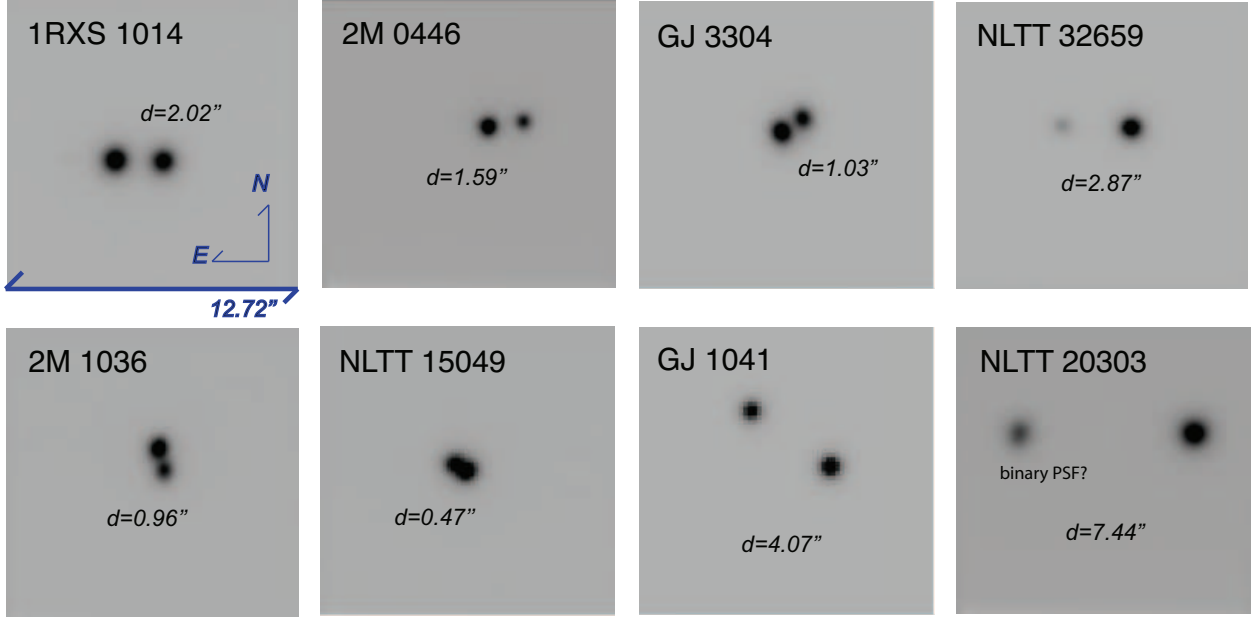


Fig. 12.— ‘Lucky’ images of the 8 VBs observed with CAPSCam. See text and Table 6 for more details on each binary pair.

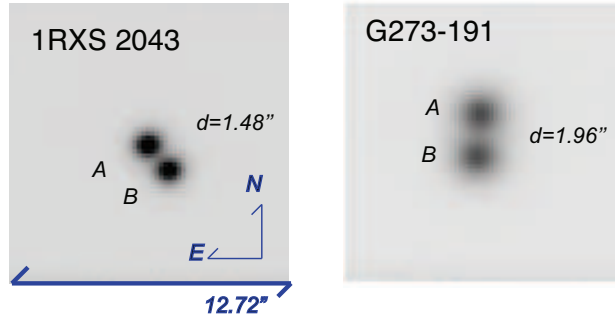


Fig. 13.— Images of 2 VBs for which the lucky imaging technique does not work due to their near-equal fluxes.

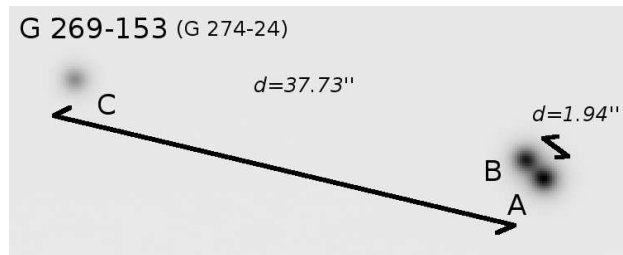


Fig. 14.— Image of G 269-153 ABC observed on UT20090909.

Table 1. Observed M Dwarfs

Name ^a	RA & DEC (2MASS) J2000	SpT ^b M–	I_{USNO} mag	$I - K_s$ mag	μ_{RA} mas yr ⁻¹	μ_{DEC} mas yr ⁻¹	μ^c Ref.	RV km s ⁻¹	D _{phot} ^d pc	D _{trig} pc
2MASS J00034227-2822410	00 03 42.28 -28 22 41.0	7.0	15.7	3.7	266 ± 10	-134 ± 10	1	11.6 ± 1.1	31 ± 3	36.1 ± 3.9
G 217-32 (AB)	00 07 42.64 +60 22 54.3	3.8	10.3	2.3	342 ± 5	-29 ± 5	2	2.7 ± 0.6	14 ± 3	–
LP 348-40	00 11 53.03 +22 59 04.8	3.5	10.2	2.2	146 ± 7.5	-229 ± 5	2	-45.2 ± 0.4	10 ± 3	–
NLTT 614	00 12 57.17 +50 59 17.3	6.4	13.7	3.1	252 ± 5	32 ± 5	2	3.0 ± 0.3	16 ± 3	–
1RXS J001557.5-163659 (AB)	00 15 58.08 -16 36 57.9	4.1	10.5	2.6	-128 ± 10	16 ± 10	3	21.0 ± 0.8	13 ± 3	18.0 ± 0.4
GJ 1006 A	00 16 14.56 +19 51 38.6	3.6	–	–	714 ± 11	-757 ± 8	4	-28.3 ± 0.3	8 ± 3	20.0 ± 4.0
GJ 3030	00 21 57.81 +49 12 38.0	2.4	10.1	1.9	204 ± 7.5	-31 ± 6.7	2	-10.8 ± 0.2	25 ± 9	–
GJ 3036 (AB) ^e	00 28 53.92 +50 22 33.0	3.7	10.3	2.3	423 ± 7.5	124 ± 6.7	2	6.3 ± 0.6	18 ± 5	–
NLTT 1875	00 35 4.88 +59 53 08.0	4.3	12.6	2.4	224 ± 7.5	-17 ± 6.7	2	-1.0 ± 0.1	26 ± 6	–
G 69-32	00 54 48.03 +27 31 03.6	4.6	11.6	2.1	338 ± 5	14 ± 5	2	7.3 ± 0.2	16 ± 3	25.6 ± 0.8
G 132-51 B (W)	01 03 42.11 +40 51 15.8	2.6	10.3	1.8	132 ± 5	-164 ± 5	2	-10.6 ± 0.3	41 ± 15	29.9 ± 2.0
G 132-51 B (E)	01 03 42.11 +40 51 15.8	3.8	10.3	1.8	132 ± 5	-164 ± 5	2	-10.9 ± 0.4	21 ± 5	29.9 ± 2.0
G 269-153 A (NE)	01 24 27.68 -33 55 08.6	4.3	10.5	2.2	178 ± 20	-110 ± 20	3	19.4 ± 2.7	16 ± 4	25.1 ± 1.0
G 269-153 B (SW)	01 24 27.79 -33 55 07.2	4.6	10.5	2.2	178 ± 20	-110 ± 20	3	18.4 ± 1.0	14 ± 3	25.1 ± 1.0
G 269-153 C (E) ^f	01 24 30.61 -33 55 01.5	5.0	–	–	160 ± 20	-112 ± 20	1,3	18.3 ± 0.5	–	25.1 ± 1.0
G 172-56	01 29 12.57 +48 19 35.5	5.4	12.1	2.0	214 ± 5	-22 ± 5	2	11.8 ± 0.4	18 ± 3	–
2MASS J01351393-0712517	01 35 13.93 -07 12 51.8	4.3	10.5	2.4	96 ± 10	-50 ± 10	3	11.7 ± 5.3	10 ± 3	37.9 ± 2.4
G 271-110	01 36 55.17 -06 47 37.9	3.5	11.0	2.2	174 ± 10	-106 ± 10	3	12.2 ± 0.4	21 ± 6	24.0 ± 0.4 ^h
1RXS J015027.1-185134	01 50 27.12 -18 51 36.0	5.4	13.3	2.6	35 ± 5	-285 ± 22	1,3	20.1 ± 0.4	24 ± 4	32.8 ± 2.7
NLTT 6549 (AB)	01 58 13.61 +48 44 19.7	1.5	10.1	1.9	213 ± 7.5	-41 ± 6.7	3	14.2 ± 0.4	44 ± 18	–
GJ 1041 A (SW)	01 59 12.39 +03 31 09.2	0.6	9.8	2.7	257.6 ± 4	24.96 ± 4	4	-7.7 ± 0.2	41 ± 16	21.5 ± 1.8
GJ 1041 Bab (NE)	01 59 12.61 +03 31 11.4	2.2+3.0 ^g	9.8	2.7	257.6 ± 4	24.96 ± 4	4	-8.5 ± 0.7	–	23.5 ± 0.8
GJ 82	01 59 23.5 +58 31 16.2	4.2	11.1	4.2	323 ± 5	-194 ± 5	2	-9.6 ± 0.3	6 ± 3	20.0 ± 4.0
GJ 3136	02 08 53.6 +49 26 56.6	2.9	9.6	2.0	234 ± 7.5	-284 ± 6.7	2	-8.1 ± 1.7	15 ± 6	–
1RXS J021836.6+121902	02 18 36.55 +12 18 58.0	1.9	9.9	2.0	149 ± 7.5	-103 ± 6.7	2	27.0 ± 0.1	29 ± 9	–
GJ 3150	02 19 2.29 +23 52 55.1	3.6	10.9	1.9	296 ± 5	-74 ± 5	2	15.7 ± 0.7	20 ± 5	–
1RXS J022735.8+471021	02 27 37.26 +47 10 04.5	4.6	11.5	2.0	119 ± 5	-183 ± 5	2	-6.0 ± 0.7	16 ± 3	–
1RXS J023138.7+445640	02 31 39.27 +44 56 38.8	4.4	11.1	2.0	72 ± 10	-68 ± 10	3	-4.7 ± 3.8	16 ± 4	–
G 36-26	02 36 44.13 +22 40 26.5	5.9	11.4	2.2	-34 ± 5	-378 ± 5	2	-3.4 ± 1.0	10 ± 3	–
GJ 3174	02 39 17.35 +07 28 17.0	3.7	11.0	2.0	486 ± 7.5	-146 ± 6.7	2	1.4 ± 0.6	20 ± 6	19.4 ± 1.1
LP 247-13	03 15 37.83 +37 24 14.3	2.7	10.5	2.1	204 ± 10	-92 ± 10	3,12	27.5 ± 0.5	28 ± 6	34.4 ± 0.6
G 246-33	03 19 28.73 +61 56 04.6	4.1	10.9	2.3	225 ± 5	-194 ± 5	2	15.4 ± 0.8	14 ± 4	–
1RXS J032230.7+285852	03 22 31.66 +28 58 29.2	4.0	11.9	2.0	150 ± 5	-49 ± 5	2,12	29.2 ± 0.3	26 ± 6	46.7 ± 1.1
2MASS J03350208+2342356	03 35 2.09 +23 42 35.6	8.5	–	–	54 ± 10	-56 ± 10	3	15.5 ± 1.7	–	42.4 ± 2.3

Table 1—Continued

Name ^a	RA & DEC (2MASS) J2000	SpT ^b M–	I_{USNO} mag	$I - K_s$ mag	μ_{RA} mas yr ⁻¹	μ_{DEC} mas yr ⁻¹	μ^c Ref.	RV km s ⁻¹	D_{phot}^d pc	D_{trig}^d pc
1RXS J034231.8+121622	03 42 31.83 +12 16 22.6	5.2	11.2	1.9	188 ± 7.5	-9 ± 6.7	2	35.4 ± 0.4	13 ± 3	–
G 80-21	03 47 23.33 -01 58 19.5	2.8	9.1	2.2	185.5 ± 5	-273.58 ± 5	4	18.9 ± 0.5	13 ± 5	15.9 ± 0.8
II Tau (SB1?)	03 49 43.25 +24 19 04.7	4.6	10.7	1.7	128 ± 10	-44 ± 10	3,12	36.8 ± 1.4^r	18 ± 3	38.3 ± 0.7
1RXS J041325.8-013919 (AB) ^e	04 13 25.76 -01 39 41.7	5.3	16.8	–	132 ± 10	-6 ± 10	3	31.7 ± 0.3	–	26.2 ± 1.7
1RXS J041417.0-090650	04 14 17.3 -09 06 54.4	4.3	11.1	2.4	96 ± 10	-138 ± 10	3	23.4 ± 0.3	22 ± 5	23.8 ± 1.4
GJ 3287	04 27 41.3 +59 35 16.7	3.8	11.3	2.2	119 ± 5	-200 ± 5	2	17.1 ± 0.6	20 ± 5	–
GJ 3305 (AB) ^e	04 37 37.46 -02 29 28.3	1.1	–	–	46.1 ± 10	-64.8 ± 10	3	21.7 ± 0.3	22 ± 9	$29.8^h \pm 0.8$
GJ 3304 A (SE)	04 38 12.56 +28 13 00.1	4.6	9.9	2.5	392 ± 6	-88 ± 3	5	35.7 ± 1.2	8 ± 3	18.7 ± 1.7
GJ 3304 B (NW) ^f	04 38 12.56 +28 13 00.1	5 ⁱ	–	–	–	–	–	–	–	18.7 ± 1.7
NLTT 13728	04 40 23.25 -05 30 08.3	6.0	13.6	4.1	225 ± 5	90 ± 6	6	29.9 ± 0.2	–	9.5 ± 0.3
NLTT 13837	04 44 8.15 +14 01 22.9	4.3	11.0	2.0	-119 ± 7	-165 ± 5	2	-13.9 ± 1.1	15 ± 3	26.0 ± 2.0
NLTT 13844	04 45 5.62 +43 24 34.2	4.6	13.2	3.2	388 ± 5	-638 ± 5	2	62.9 ± 0.2	20 ± 4	–
2MASS J04465175-1116476 A (E)	04 46 51.75 -11 16 47.6	4.9	9.6	2.3	-154 ± 10	-50 ± 10	1,3	14.9 ± 0.3	8 ± 3	18.7 ± 1.7
2MASS J04465175-1116476 B (W) ^f	04 46 51.75 -11 16 47.6	6 ⁱ	–	–	-154 ± 10	-50 ± 10	–	–	–	–
2MASS J04472312-2750358	04 47 23.13 -27 50 35.8	0.5	8.4	1.6	67 ± 5	171.9 ± 5	3	30.0 ± 0.2	20 ± 3	∞ –
G 81-34 (AB)	04 49 29.47 +48 28 45.9	4.0	10.6	2.4	180 ± 5	-195 ± 5	2	25.2 ± 0.3	15 ± 4	–
1RXS J045101.0+312734	04 51 1.38 +31 27 23.9	3.7	10.3	2.1	198 ± 10	-41 ± 10	3	27.6 ± 0.2	13 ± 4	–
NLTT 14116	04 52 24.41 -16 49 21.9	3.3	9.1	2.2	118 ± 5	-211 ± 5	2	27.9 ± 0.3	13 ± 4	16.3 ± 0.4
GJ 3335	05 09 9.97 +15 27 32.5	3.5	10.2	2.2	142 ± 5	-626 ± 5	5	-16.2 ± 0.8	14 ± 4	28.2 ± 2.0
NLTT 15049 A (SW)	05 25 41.67 -09 09 12.3	3.8	9.9	2.3	40 ± 10	-189.7 ± 10	3	28.4 ± 0.5	11 ± 3	20.7 ± 2.2
NLTT 15049 B (NE) ^f	05 25 41.67 -09 09 12.3	5 ⁱ	9.9	2.3	–	–	–	–	–	20.7 ± 2.2
GJ 207.1	05 33 44.81 +01 56 43.4	2.0	9.1	2.2	-225 ± -239	-158 ± -156	5	64.5 ± 0.65^p	17 ± 6	16.1 ± 0.8
1RXS J055446.0+105559	05 54 45.74 +10 55 57.1	2.1	10.2	2.3	-140 ± -134	-74 ± -67	2	14.2 ± 2.1	27 ± 9	25.4 ± 1.9
2MASS J05575096-1359503	05 57 50.97 -13 59 50.3	7.0	16.5	4.8	55.57 ± 10	-162.89 ± 10	3	30.3 ± 2.8	60 ± 12	526 ± 277
GJ 3372 B	05 59 55.69 +58 34 15.6	4.2	10.5	2.3	9 ± 7.5	-258 ± 6.7	2	0.2 ± 0.6	11 ± 3	–
G 249-36	06 05 29.36 +60 49 23.2	4.9	10.7	2.6	296 ± 5	-792 ± 5	2	128.5 ± 2.6	8 ± 3	–
CD-35 2722 (AB) ^l	06 09 19.2 -35 49 30.6	1.0	–	–	-4.6 ± 1.9	-59.8 ± 1.6	7	31.4 ± 1.0	–	22.7 ± 1.0
GJ 3395	06 31 1.16 +50 02 48.6	0.8	9.4	2.3	-107 ± 10	-163 ± 10	3	8.6 ± 0.2	28 ± 9	–
G 108-36	06 51 59.02 +03 12 55.3	2.5	10.3	2.0	-213 ± 7.5	-46 ± 6.7	2	42.2 ± 0.1	27 ± 11	22.2 ± 0.6
GJ 3417 A (NE)	06 57 57.04 +62 19 19.7	5.2	10.3	2.6	320 ± 5	-512 ± 5	2	17.6 ± 0.6	9 ± 3	$11.4^j \pm 0.3$
BD+20 1790 ^l	07 23 43.592 +20 24 58.7	-1.0	8.9	2.0	-65.8 ± 3	-228 ± 3	7	8.25 ± 0.8^k	–	25.8 ± 1.3
GJ 2060 A	07 28 51.38 -30 14 49.1	1.3	8.4	2.7	-130.77 ± 2.14	-130.94 ± 2.71	4	30.1 ± 1.3	15 ± 6	15.7 ± 0.5
GJ 2060 B	07 28 51.39 -30 14 49.2	1.5	–	–	-130.77 ± 2.14	-130.94 ± 2.71	–	–	–	15.7 ± 0.5
GJ 2060 C	07 25 51.18 -30 15 52.8	5.0	–	–	-130 ± 10	-180 ± 10	1	–	–	14.9 ± 0.7

Table 1—Continued

Name ^a	RA & DEC (2MASS) J2000	SpT ^b M–	I_{USNO} mag	$I - K_s$ mag	μ_{RA} mas yr ⁻¹	μ_{DEC} mas yr ⁻¹	μ^c Ref.	RV km s ⁻¹	D _{phot} ^d pc	D _{trig} pc
GJ 277 B	07 31 57.35 +36 13 47.8	3.3	–	–	-252.9 ± 1.5	-257 ± 1.4	4	-0.7 ± 0.1	–	11.5 ± 0.6
1RXS J073829.3+240014	07 38 29.52 +24 00 08.8	2.7	10.3	2.2	-179 ± 5	-107 ± 5	1,2	16.9 ± 0.2	–	18.9 ± 0.9
NLTT 18549	07 52 23.9 +16 12 15.7	7.0	–	–	182 ± 7.5	-359 ± 6.7	3	-14.7 ± 0.2	12 ± 3	18.6 ± 1.1
2MASS J07572716+1201273	07 57 27.16 +12 01 27.3	2.3	10.0	1.8	-134 ± 19	-290 ± 20	2	29.4 ± 0.1	18 ± 3	22.9 ± 1.0
2MASS J08031018+2022154	08 03 10.18 +20 22 15.5	3.3	10.3	2.0	-104 ± 10	-58 ± 10	3	35.5 ± 1.5	18 ± 6	–
GJ 316.1	08 40 29.75 +18 24 09.2	6.0	13.5	3.4	-799 ± 10	-454 ± 10	1,8	65.8 ± 0.1	15 ± 3	13.5 ± 0.5
NLTT 20303 A (W)	08 48 36.45 -13 53 08.4	2.6	–	–	-180 ± 8	5 ± 11	1,3	21.0 ± 1.6	26 ± 8	23.3 ± 1.4
NLTT 20303 B (E) ^f	08 48 36.45 -13 53 08.4	3.5 ⁱ	–	–	-180 ± 8	5 ± 11	–	–	–	23.5 ± 1.4
LP 726-13 ^m	08 48 39.18 -13 54 06.4	–	–	–	-314 ± 5	-4 ± 5	1,6	–	–	32.9 ± 2.4
1RXS J091744.5+461229 (AB)	09 17 44.73 +46 12 24.7	1.7	–	–	-128.5 ± 10	-19 ± 10	3	-7.2 ± 0.9	32 ± 9	–
G 43-2	09 48 50.2 +15 38 44.9	2.0	–	–	-9 ± 5	217 ± 5	2	-0.8 ± 0.2	–	17.6 ± 1.0
NLTT 22741	09 51 4.6 +35 58 09.8	4.5	11.9	2.2	-106 ± 10	-171 ± 10	2,3	10.2 ± 0.2	19 ± 3	–
GJ 3577 A (W)	09 59 18.8 +43 50 25.6	3.5	10.7	1.9	-100 ± 10	-218 ± 10	3	-1.7 ± 1.3	29 ± 9	–
G 196-3 A	10 04 21.49 +50 23 13.6	3.0	10.7	3.5	-127 ± 7.5	-183 ± 6.7	2,3	-0.7 ± 1.2	11 ± 4	+
GJ 2079 (AB, SB1?)	10 14 19.19 +21 04 29.8	0.7	8.2	2.0	-144 ± 1.1	-154 ± 1.3	4	8.7 ± 1.8 ^r	34 ± 13	23.1 ± 1.1
1RXS J101432.0+060649 A (E)	10 14 31.95 +06 06 41.0	4.1	9.9	2.0	-150 ± 5	-66 ± 5	1,2,5	16.6 ± 1.7	14 ± 3	40.5 ± 8.2
1RXS J101432.0+060649 B (W) ^f	10 14 31.95 +06 06 41.0	4.5 ⁱ	9.9	1.9	-150 ± 5	-66 ± 5	–	–	–	40.4 ± 8.2
GJ 388	10 19 36.35 +19 52 12.2	3.5	7.8	3.2	-502 ± 2.8	-43 ± 2.6	7	12.5 ± 0.2	3 ± 3	4.9 ^j ± 0.1
G 44-9	10 20 44.07 +08 14 23.4	5.9	12.1	2.7	-244 ± 5	-6 ± 5	1,2	14.1 ± 0.4	12 ± 3	37.7 ± 2.1
2MASS J10364483+1521394 A (N)	10 36 44.84 +15 21 39.5	4.0	10.0	2.1	102 ± 10	-60 ± 10	1,3	-12.7 ± 0.2	12 ± 3	20.1 ± 2.0
2MASS J10364483+1521394 Bab (S) ^f	10 36 44.84 +15 21 39.5	4.5+4.5 ⁿ	–	–	102 ± 3	-60 ± 2	–	–	–	20.1 ± 2.0
GJ 3629 (AB)	10 51 20.6 +36 07 25.6	3.0	10.6	2.1	-188 ± 5	-56 ± 6	2	13.0 ± 0.3	22 ± 7	–
GJ 3639	11 03 10 +36 39 08.5	3.5	10.4	1.8	-196 ± 5	27 ± 5	2	-10.0 ± 0.3	18 ± 6	–
NLTT 26114	11 03 21.25 +13 37 57.1	3.0	10.0	2.1	-188 ± 5	68 ± 5	1,2	-18.1 ± 0.1	16 ± 5	15.4 ± 0.7
G 119-62	11 11 51.76 +33 32 11.2	3.5	9.7	2.2	-172 ± 10	122 ± 10	3	2.2 ± 0.2	11 ± 3	14.6 ^j ± 2.7
1RXS J111300.1+102518	11 13 0.6 +10 25 05.9	3.0	11.4	2.2	122 ± 10	-134 ± 10	1,3	-16.7 ± 0.9	28 ± 9	23.0 ± 1.6
GJ 3653	11 15 54.04 +55 19 50.6	0.5	9.6	2.3	-171 ± 2.8	-96 ± 2.6	7	-7.6 ± 0.8	34 ± 12	–
2MASS J11240434+3808108	11 24 4.35 +38 08 10.9	4.5	10.6	1.6	134 ± 12	-18 ± 8	2	-11.5 ± 0.5	15 ± 3	–
G 10-52	11 48 35.49 +07 41 40.4	3.5	10.6	2.0	142 ± 10	-168 ± 10	1,3	-9.8 ± 0.8	19 ± 7	20.7 ± 0.9
G 122-74	12 12 11.36 +48 49 03.2	3.5	10.0	1.6	208 ± 5	-316 ± 5	2	-22.3 ± 0.1	–	–
GJ 3729 (AB)	12 29 2.9 +41 43 49.7	3.5	9.9	1.9	-196 ± 5	-222 ± 5	2	-1.7 ± 0.3	17 ± 5	–
GJ 3730	12 29 27.13 +22 59 46.7	4.0	11.0	2.0	-166 ± 10	-14 ± 10	1,3	-22.6 ± 0.1	16 ± 4	20.4 ± 1.2
1RXS J124147.5+564506	12 41 47.37 +56 45 13.8	2.5	10.4	1.8	120 ± 10	0 ± 10	11,12	-8.7 ± 0.2	30 ± 11	–
GJ 490 B (ab)	12 57 39.35 +35 13 19.5	4.0	–	–	-269 ± 7.5	-149 ± 6.7	10	-5.7 ± 0.50 ^q	14 ± 3	18.1 ± 1.0

Table 1—Continued

Name ^a	RA & DEC (2MASS) J2000	SpT ^b M–	I_{USNO} mag	$I - K_s$ mag	μ_{RA} mas yr ⁻¹	μ_{DEC} mas yr ⁻¹	μ^c Ref.	RV km s ⁻¹	D_{phot}^d pc	D_{trig} pc
GJ 490 A	12 57 40.3 +35 13 30.6	0.5	8.8	2.3	-269 ± 5	-149 ± 5	2	-2.9 ± 0.6	24 ± 10	18.1 ± 1.0
NLTT 32659 A (W)	13 02 5.87 +12 22 21.6	1.6	10.0	1.7	-225 ± 5	-103 ± 5	2	-0.1 ± 0.8	40 ± 11	–
NLTT 32659 B (E)	13 02 5.87 +12 22 21.6	3.7	10.0	1.7	-225 ± 5	-103 ± 5	2	0.8 ± 0.7	–	–
GJ 1167 A	13 09 34.95 +28 59 06.6	4.8	11.1	2.5	-332 ± 5	-210 ± 5	2	-5.2 ± 2.6	11 ± 3	11.5 ^j ± 2.4
GJ 3786 (AB) ^e	13 27 19.67 -31 10 39.4	3.5	10.9	2.4	-565 ± 5	-151 ± 5	6	7.3 ± 0.8	27 ± 11	20.0 ± 1.0
2MASS J13292408-1422122	13 29 24.08 -14 22 12.3	2.8	10.4	2.2	110 ± 6	-42 ± 5	3	-1.8 ± 0.2	21 ± 5	–
2MASS J14215503-3125537 (AB)	14 21 55.04 -31 25 53.7	3.9	11.0	2.2	-166 ± 5	-48 ± 5	1,3	-26.5 ± 0.3	22 ± 4	40.0 ± 2.4
2MASS J1442809-0424078	14 44 28.1 -04 24 07.8	3.0	11.0	2.1	118 ± 10	-96 ± 10	3	8.1 ± 0.9	29 ± 10	–
1RXSJ150907.2+590422	15 09 8.09 59 04 25.9	2.2	9.7	1.2	86 ± 10	-52 ± 10	3	-5.0 ± 0.3	33 ± 11	–
GJ 9520	15 21 52.92 +20 58 39.5	1.0	7.8	2.1	78.5 ± 0.9	130.4 ± 0.7	4	6.9 ± 0.5	14 ± 5	11.4 ± 0.3
NLTT 40561	15 33 50.62 +25 10 10.6	3.5	11.3	1.7	18 ± 5	-232 ± 5	5	12.5 ± 0.7	29 ± 10	–
G 167-54	15 43 48.48 +25 52 37.7	4.1	11.3	2.1	-171 ± 10	317 ± 10	2,3	-40.0 ± 0.1	13 ± 3	–
2MASS J15534211-2049282 A (S)	15 53 42.12 -20 49 28.2	3.4	13.4	3.8	-8 ± 10	-22 ± 10	3	-6.7 ± 2.4	145 ± 29	333.3 ± 77.8
GJ 3928 (AB) ^e	15 55 31.78 +35 12 02.9	5.3	10.5	2.5	-226 ± 10	156 ± 10	3	-15.5 ± 0.7	8 ± 3	–
NLTT 43695 (E)	16 51 9.95 +35 55 07.1	4.6	11.7	2.2	-70 ± 10	176 ± 10	3	-37.6 ± 0.2	22 ± 4	–
LP 331-57 (AB) ^e	17 03 52.83 +32 11 45.6	2.4	10.9	3.9	188.4 ± 3.9	97.6 ± 2.2	7	-5.5 ± 0.5	17 ± 7	–
2MASS J17073334+4301304	17 7 33.3 +43 1 30	10.0	–	–	-200 ± 1.25	-22 ± 1.56	9	-10.8 ± 0.7	–	–
GJ 669 B (W)	17 19 52.98 +26 30 02.6	5.6	9.6	2.2	-217 ± 7.5	354 ± 6.7	2	-34.6 ± 0.2	5 ± 3	11.8 ± 0.7
GJ 669 A (E)	17 19 54.22 +26 30 03.0	3.4	8.8	2.4	-210.7 ± 1.2	353.5 ± 1.2	4	-34.9 ± 0.1	5 ± 3	11.7 ± 0.7
1RXS J173130.9+272134	17 31 29.75 +27 21 23.3	10 ^o	14.9	4.0	-82 ± 7.5	-240 ± 6.7	5	-29.3 ± 0.4	–	–
G 227-22	18 02 16.6 +64 15 44.6	6.1	9.9	2.3	206 ± 5	-386 ± 5	2	-1.2 ± 0.2	5 ± 3	–
GJ 4044	18 13 6.57 +26 01 51.9	4.5	10.4	2.3	218 ± 7.5	-36 ± 6.7	3	-8.8 ± 0.3	10 ± 3	17.2 ± 0.7
1RXS J183203.0+203050 A (N)	18 32 2.91 +20 30 58.1	4.9	11.5	1.7	-46 ± 5	-202 ± 5	2	-18.1 ± 0.3	28 ± 4	–
1RXS J183203.0+203050 B (S)	18 32 2.91 +20 30 58.1	5.1	11.5	1.7	-46 ± 10	-202 ± 10	3	-19.5 ± 0.5	28 ± 4	–
1RXS J184410.0+712909 A (E)	18 44 10.2 +71 29 17.6	3.9	10.7	2.0	28 ± 10	146 ± 10	3	-18.8 ± 3.3	22 ± 5	–
1RXS J184410.0+712909 B (W)	18 44 10.2 +71 29 17.6	4.1	10.7	2.0	28 ± 10	146 ± 10	3	-17.4 ± 1.5	22 ± 5	–
GJ 9652 A (SB1?)	19 14 39.26 +19 19 02.6	4.5	10.5	3.6	-617.4 ± 2.5	433.2 ± 2.7	4	-80.9 ± 0.9 ^f	5 ± 3	19.1 ± 1.0
2MASS J19303829-1335083	19 30 38.3 -13 35 08.4	6.0	13.6	3.0	167 ± 5	359 ± 5	1,2	-21.4 ± 0.1	19 ± 3	27.7 ± 1.2
1RXS J193124.2-213422	19 31 24.34 -21 34 22.6	2.4	10.2	2.4	58 ± 10	-100 ± 10	1,3	-26.0 ± 1.8	22 ± 9	26.0 ± 2.0
1RXS J193528.9+374605 (SB1?)	19 35 29.23 +37 46 08.2	3.0	9.9	3.2	-136.4 ± 10	-98.6 ± 10	3	-33.3 ± 0.3 ^f	10 ± 4	–
1RXS J194213.0-204547	19 42 12.82 -20 45 47.8	5.1	11.1	2.3	-16 ± 6	-130 ± 7	5	-1.7 ± 0.2	10 ± 3	16.3 ± 0.4
G 125-36	19 50 15.93 +31 46 59.9	2.1	10.3	2.0	177 ± 5	329 ± 5	2,3	-29.6 ± 0.1	21 ± 3	–
2MASS J20003177+5921289 (AB)	20 00 31.77 +59 21 29.0	4.1	10.0	1.2	-128 ± 18	-66 ± 15	3	-5.2 ± 0.9	20 ± 5	–
1RXS J204340.6-243410 A (NE)	20 43 41.15 -24 33 53.5	3.7	10.1	2.3	62 ± 10	-60 ± 10	3	-5.0 ± 0.6	13 ± 3	28.1 ± 3.9

Table 1—Continued

Name ^a	RA & DEC (2MASS) J2000	SpT ^b M–	I_{USNO} mag	$I - K_s$ mag	μ_{RA} mas yr ⁻¹	μ_{DEC} mas yr ⁻¹	μ^c Ref.	RV km s ⁻¹	D_{phot}^d pc	D_{trig} pc
1RXS J204340.6-243410 B (SW)	20 43 41.15 -24 33 53.5	4.1	10.1	2.3	62 ± 10	-60 ± 10	3	-6.0 ± 0.9	13 ± 3	28.1 ± 3.9
NLTT 49856	20 46 43.61 -11 48 13.2	4.5	10.9	2.5	342 ± 5	-60 ± 5	1,6	-32.8 ± 0.3	12 ± 3	18.7 ± 0.5
2MASS J20530910-0133039	20 53 9.1 -01 33 04.0	5.6	11.4	1.6	354 ± 5	-218 ± 2	10	-41.1 ± 0.8	14 ± 3	18.2 ± 0.7
NLTT 50066 (AB)	20 53 14.65 -02 21 21.9	2.9	10.7	2.2	186 ± 5	15 ± 5	6	-39.9 ± 1.1	32 ± 13	37.9 ± 5.7
GJ 4185 B	21 16 3.79 +29 51 46.0	3.3	10.5	2.0	208 ± 10	42 ± 10	3	-2.3 ± 0.3	18 ± 6	19.3 ± 1.1
GJ 4185 A (ab)	21 16 5.77 +29 51 51.1	3.3	9.8	2.2	206 ± 10	34 ± 10	3	-1.8 ± 0.6	17 ± 5	19.5 ± 1.1
GJ 4231	21 52 10.4 +05 37 35.7	2.4	–	–	119.17 ± 1.5	-150.29 ± 1.4	4	-15.1 ± 1.5	18 ± 7	31.8 ± 4.8
1RXS J221419.3+253411 (AB)	22 14 17.66 +25 34 06.6	4.3	11.3	2.0	164 ± 5	-44 ± 5	5	-19.9 ± 0.3	21 ± 4	28.7 ± 2.1
GJ 4282 A (E)	22 33 22.65 -09 36 53.8	2.5	9.9	2.2	140 ± 10	14 ± 10	3	-4.4 ± 1.4	29 ± 11	–
GJ 4282 B (W)	22 33 22.65 -09 36 53.8	2.6	9.9	2.2	140 ± 5	14 ± 5	2	-3.7 ± 1.0	29 ± 11	–
2MASS J22344161+4041387	22 34 41.62 +40 41 38.8	6.0	14.2	2.8	-1.85 ± 10	-3.25 ± 10	3	-10.9 ± 0.7	325 ± 65	–
LP 984-92 ^f	22 45 0.05 -33 15 25.8	4.5	9.3	2.4	184.7 ± 2.6	-119.7 ± 2.3	4	–	8 ± 3	22.0 ± 1.4
LP 984-91	22 44 57.94 -33 15 01.6	4.0	9.3	2.4	184.7 ± 2.6	-119.7 ± 2.3	4	3.2 ± 0.5	8 ± 3	22.5 ± 1.5
GJ 873	22 46 49.81 +44 20 03.1	3.2	8.9	3.6	-706 ± 2.8	-460 ± 2.6	4	0.0 ± 0.2	5 ± 3	5.0 ± 0.1
NLTT 54873	22 47 37.64 +40 41 25.4	3.8	11.4	1.9	166 ± 5	92 ± 5	2	-3.0 ± 0.9	22 ± 5	–
GJ 875.1	22 51 53.49 +31 45 15.3	2.7	10.5	3.6	523 ± 2.8	-52 ± 2.6	4	-2.5 ± 0.4	13 ± 5	14.2 ± 0.5
2MASS J22581643-1104170	22 58 16.43 -11 04 17.1	2.7	10.3	2.0	112 ± 6	-4 ± 5	1,2	16.0 ± 0.2	24 ± 9	31.1 ± 2.9
GJ 9809	23 06 4.83 +63 55 34.0	0.3	9.6	2.6	171.4 ± 2.8	-58.55 ± 2.6	4	-23.2 ± 0.4	21 ± 3	24.9 ± 0.9
NLTT 56194	23 13 47.28 +21 17 29.4	7.5	13.0	2.6	256 ± 5	-30 ± 5	2	-1.6 ± 0.3	14 ± 3	–
NLTT 56566 (AB) ^e	23 20 57.66 -01 47 37.3	3.8	10.8	2.3	168 ± 5	26 ± 5	6	-7.2 ± 0.4	17 ± 5	41.0 ± 2.7
GJ 4338 B (ab)	23 29 22.58 +41 27 52.2	4.2	–	–	415 ± 7.5	-41 ± 6.7	2	-14.5 ± 0.5	9 ± 3	14.8 ^j ± 0.4
GJ 4337 A	23 29 23.46 +41 28 06.9	2.9	10.0	2.9	415 ± 7.5	-41 ± 6.7	2	-15.2 ± 0.6	12 ± 5	14.8 ^j ± 2.2
GJ 1290	23 44 20.84 +21 36 05.0	3.4	10.4	2.2	452 ± 5	86 ± 3	2	-5.9 ± 0.4	16 ± 5	–
1RXS J235005.6+265942	23 50 6.39 +26 59 51.9	4.0	11.2	1.9	181 ± 5	-49 ± 5	2	-0.7 ± 2.8	19 ± 4	–
G 68-46	23 51 22.28 +23 44 20.8	4.0	10.8	2.0	265 ± 5	-74 ± 4	2	-2.1 ± 0.5	15 ± 3	–
1RXS J235133.3+312720 (AB) ^e	23 51 33.67 +31 27 23.0	2.0	10.9	2.0	108 ± 10	-84 ± 10	3	-13.5 ± 0.6	45 ± 16	–
1RXS J235452.2+383129	23 54 51.47 +38 31 36.3	3.1	10.2	2.1	-134 ± 5	-86 ± 5	2	5.6 ± 0.3	17 ± 6	–
GJ 4381 (AB)	23 57 49.9 +38 37 46.9	2.8	9.9	2.0	-125 ± 5	-138 ± 5	2	-3.8 ± 0.4	21 ± 8	–
G 273-191 A (N)	23 58 13.66 -17 24 33.8	1.9	9.7	2.3	217 ± 5	14 ± 5	6	-8.7 ± 1.8	33 ± 10	39.1 ± 5.3
G 273-191 B (S)	23 58 13.66 -17 24 33.8	1.9	9.7	2.3	217 ± 5	14 ± 5	6	-8.7 ± 1.8	33 ± 10	39.0 ± 5.3
G 130-31	23 59 19.86 +32 41 24.5	5.6	11.8	2.2	-174 ± 5	-241 ± 5	2	-52.3 ± 0.2	13 ± 3	–

^aThose target names with notations in parentheses were resolved as visual binaries (VB) and when possible, both components were observed. Targets resolved as VBs using adaptive optics imaging are designated by “(AB)” or “(ab)”. The tabulated spectroscopy and astrometry are composites of both components. Those that are RV variable are

labeled as potential single-line spectroscopic binaries (SB1).

^bThe SpTs are from SLR09 with uncertainties of ± 0.5 subclasses.

^cReferences for the proper motions are: (1) this work; (2) Lépine & Shara (2005); (3) Monet et al. (2003); (4) Perryman & ESA (1997); (5) Zacharias et al. (2004); (6) Salim & Gould (2003); (7) Høg et al. (2000); (8) van Altena et al. (1995); (9) Jameson et al. (2008); (10) Kharchenko et al. (2002); (11) Reid et al. (2007a); (12) Zacharias et al. (2005).

^dPhotometric distances are calculated using the Baraffe et al. (1998) models and the SLR09 age range (Column 11 of Table 5). We also account for known binarity.

^eGJ 3036: $0.426''$ VB (Daemgen et al. 2007), 1RXS J0413: $0.79''$ VB (McCarthy et al. 2001), GJ 3305: $0.27''$ VB (Kasper et al. 2007; Delorme et al. 2012); GJ 3786: $0.544''$ VB (Daemgen et al. 2007), GJ 3928: $1.571''$ VB (Daemgen et al. 2007), LP 331-57: $1.13''$ VB (Daemgen et al. 2007), NLTT 56566: $0.099''$ VB (Daemgen et al. 2007), 1RXS J2351: $2.4''$ VB (Bowler et al. 2012)

^fCommon proper motion companion found in parallax program.

^gReported to be a spectroscopic binary by Shkolnik et al. (2010).

^hDistance adopted from Hipparcos distance of common proper motion companions: 51 Eri for GJ 3305 and EX Cet for G271-110.

ⁱSpT estimated from flux ratio in the CAPScam image (Table 6).

^jDistance from Hipparcos (Perryman & ESA 1997).

^kRV from White et al. (2007).

^lCD-35 2722 was found to have a young brown dwarf companion (Wahhaj et al. 2011) and BD+20 1790 may host a massive close-in planet (Hernán-Obispo et al. 2010).

^mBackground high proper motion star.

ⁿFrom Daemgen et al. (2007).

^oFrom Reid et al. (2008).

^pMontes et al. (2001) report an RV of $22.1 \pm 0.1 \text{ km s}^{-1}$

^qProbably due to the binary nature of this target, its measured RV is slightly different from its companion, GJ 490 A.

^rRadial velocity variable. Here we report the mean RV of our and literature values. See Table 8 for individual velocities.

Table 2. Summary of Astrometric Observations

Name	First epoch (UT) YYYYMMDD	Last epoch (UT) YYYYMMDD	N _{epochs}	π_{rel} mas	π_{abs} mas	σ_{abs} mas	Comments
2MASS J00034227-2822410	20090909	20100114	5	27.2	27.7	3.0	PM Pair to HIP 296
1RXS J001557.5-163659 (AB)	20090908	20100818	4	55.2	55.7	1.3	-
G 69-32	20090909	20101114	4	38.6	39.1	1.2	-
G 269-153 A (NE)					39.9 ^a	1.6	Plx from C
G 269-153 B (NE)					39.9 ^a	1.6	Plx from C
G 269-153 C (E)	20090909	20101114	5	39.4	39.9	1.6	-
2MASS J01351393-0712517	20090909	20101116	4	25.9	26.4	1.7	-
1RXS J015027.1-185134	20090909	20101116	4	30.0	30.5	2.5	-
GJ 1041 A (SW)	20090909	20101114	4	46.0	46.5	4.0	-
GJ 1041 B (NE)	20090909	20101114	4	42.0	42.5	1.5	-
GJ 3174	20090126	20101114	5	51.0	51.5	3.0	-
2MASS J03350208+2342356	20090131	20101114	5	23.1	23.6	1.3	-
G 80-21	20090909	20101114	5	62.5	63	2.5	-
1RXS J041325.8-013919	20090126	20101116	5	37.7	38.2	2.5	-
1RXS J041417.0-090650	20090131	20101114	6	41.5	42	2.5	-
GJ 3304 A	20090202	20101114	4	53.0	53.5	5.0 ^a	Barely resolved VB
GJ 3304 B					53.5	5.0 ^a	Barely resolved VB
NLTT 13728	20090126	20110120	7	105.0	105.5	3.2	-
NLTT 13837	20090202	20101116	3	38.0	38.5	3.0	-
2MASS J04465175-1116476 A	20090126	20101114	6	53.1	53.6	5.0 ^a	Barely resolved VB
2MASS J04465175-1116476 B					53.6	5.0 ^a	Barely resolved VB
NLTT 14116	20090126	20101116	6	60.9	61.4	1.5	-
GJ 3335	20090202	20101116	6	34.9	35.4	2.5	-
NLTT 15049	20090201	20101116	6	47.7	48.2	5.0	-
GJ 207.1	20090201	20101114	4	61.7	62.2	3.0	-
1RXS J055446.0+105559	20090201	20110413	3	38.8	39.3	3.0	-
2MASS J05575096-1359503	20090126	20101114	4	1.4 ^a	1.9	1.0	Unreliable small plx
G 108-36	20090126	20101114	4	44.5	45	1.3	-
GJ 2060 A				75.1	75.6	3.0	Plx from C
GJ 2060 B							Plx from C
GJ 2060 C	20090126	20101114	5	66.4	66.9	3.0	-
1RXS J073829.3+240014	20090201	20110122	4	52.5	53	2.5	-
NLTT 18549	20090126	20101116	4	53.2	53.7	3.3	-
2MASS J07572716+1201273	20090201	20101114	4	43.2	43.7	2.0	-

Table 2—Continued

Name	First epoch (UT) YYYYMMDD	Last epoch (UT) YYYYMMDD	N _{epochs}	π_{rel} mas	π_{abs} mas	σ_{abs} mas	Comments
GJ 316.1	20090409	20110414	3	73.6	74.1	3.0	-
NLTT 20303 A (E)	20090126	20110413	6	42.4	42.9	2.5	-
NLTT 20303 B (W)				42.0	42.5	2.5	-
LP 726-13	20090126	20110413	6	29.9	30.4	2.2	not in SLR09
G 43-2	20090126	20110120	4	56.4	56.9	3.2	-
1RXS J101432.0+060649	20090131	20100125	3	24.2	24.7	5.0 ^a	Barely resolved VB
1RXS J101432.0+060649					24.7	5.0 ^a	Barely resolved VB
G 44-9	20090126	20100125	4	26.0	26.5	1.5	-
2MASS J10364483+1521394 A	20090126	20100125	4	49.3	49.8	5.0 ^a	Barely resolved VB
2MASS J10364483+1521394 B						5.0 ^a	Barely resolved VB
NLTT 26114	20090201	20100125	3	64.3	64.8	3.0	-
1RXS J111300.1+102518	20090201	20100127	3	42.9	43.4	3.0	-
G 10-52	20090201	20110120	6	47.7	48.2	2.2	-
GJ 3730	20090201	20100125	3	48.6	49.1	3.0	-
2MASS J12292799+2258327	20090201	20100125	3	12.0	12.5	3.0	not in SLR09
GJ 3786	20090131	20100621	4	49.6	50.1	2.5	-
2MASS J14215503-3125537	20090409	20110412	5	24.5	25	1.5	-
2MASS J15534211-2049282 (S)	20090409	20100816	5	2.5	3 ^a	0.7	Unreliable small plx
GJ 669 A	20090409	20100817	4	85.0	85.5	5.0 ^a	HIP plx is 86 mas
GJ 669 B	20090409	20100817	4	84.0	84.5	5.0 ^a	Barely resolved VB
GJ 4044	20090409	20100818	4	57.7	58.2	2.3	Excess scatter in Decl.
2MASS J19303829-1335083	20090410	20110412	6	35.6	36.1	1.5	-
1RXS J193124.2-213422	20090410	20100819	5	38.0	38.5	3.0	-
1RXS J194213.0-204547	20090409	20100819	5	60.9	61.4	1.6	Excess scatter in Decl.
1RXS J204340.6-243410 A (NE)	20090908	20100817	4	35.1	35.6	5.0 ^a	Barely resolved VB
1RXS J204340.6-243410 B (SW)					35.6	5.0 ^a	Barely resolved VB
NLTT 49856	20090909	20100819	4	53.0	53.5	1.3	-
2MASS J20530910-0133039	20090908	20100818	3	54.5	55	2	-
NLTT 50066 (AB)	20090908	20100818	4	25.9	26.4	1.5	-
NLTT 50060	20090908	20100818	4	11.4	11.9	2	-
GJ 4185B	20090909	20100819	4	51.4	51.9	3	-
GJ 4185 A (ab)	20090909	20100819	4	50.7	51.2	3	-
1RXS J221419.3+253411 (AB)	20091102	20101116	3	34.3	34.8	2.5	-
LP 984-91	20090908	20101116	4	44.0	44.5	3	-

Table 2—Continued

Name	First epoch (UT) YYYYMMDD	Last epoch (UT) YYYYMMDD	N _{epochs}	π_{rel} mas	π_{abs} mas	σ_{abs} mas	Comments
LP 984-92	20090908	20101116	4	45.0	45.5	3	-
2MASS J22581643-1104170	20090909	20100819	4	31.7	32.2	3	-
NLTT 56566	20090908	20100817	5	23.9	24.4	1.6	-
G 273-191 A (N)	20090908	20101114	5	25.1	25.6	5.0 ^a	Barely resolved VB
G 273-191 B (S)	20090908	20100818			25.6	5.0 ^a	Barely resolved VB
CD-35 2722 (AB)	20100409	20110116	4	43.6	44.1	1.2	not in SLR09
BD+20 1790	20080901	20101116	5	37.4	37.9	1.3	not in SLR09

^aBinary PSF produced a larger than normal error in parallax. We set a conservative uncertainty on these of 5 mas. See text for more details.

Table 3. Trigonometric Distances: CAPSCam vs. Hipparcos

Name	CAPSCam Distance pc	Hipparcos Distance pc
2MASS J00034227-2822410	36.10 ± 3.91	39.54 ± 1.74
GJ 1041A (SW)	21.51 ± 1.85	29.82 ± 4.71
GJ 1041Bab (NE)	23.53 ± 0.83	29.82 ± 4.71
G 80-21	15.87 ± 0.83	16.27 ± 0.80
GJ 207.1	16.08 ± 0.78	16.82 ± 1.10
GJ 316.1	13.50 ± 0.55	14.06 ± 0.20
GJ 2079 (AB)	23.09 ± 1.07	20.43 ± 0.71
GJ 699B (W)	11.83 ± 0.68	11.60 ± 0.81
GJ 669A (E)	11.70 ± 0.68	11.60 ± 0.81
LP-984-92	21.98 ± 1.45	23.61 ± 1.88
LP 984-91 A (NW)	22.47 ± 1.51	23.61 ± 1.88

Table 4. Young Moving Groups Searched for New Members

Group	U km s ⁻¹	V km s ⁻¹	W km s ⁻¹	Age Myr	Dist. pc	Ref.
AB Dor Moving Group	-8	-27	-14	50–100	15–55	Zuckerman et al. (2004); López-Santiago et al. (2006)
β Pictoris Moving Group	-11	-15	-9.5	10–12	10–50	Torres et al. (2006, 2008)
Carina Association	-10.2	-23	-4.4	30	50–120	Torres et al. (2008)
Castor Moving Group	-10.7	-8	-9.7	200	$\lesssim 45$	Montes et al. (2001)
Chamaeleon-Near Moving Group	-11	-16	-8	10	60–110	Zuckerman & Song (2004)
η Chamaeleon Cluster	-12	-19	-10	8	~ 97	Zuckerman & Song (2004)
Columba Association	-13.2	-21.8	-5.9	30	50–110	Torres et al. (2008)
Hercules-Lyra Association	-15.4	-23.4	12	200	$\lesssim 25$	López-Santiago et al. (2006)
Hyades Open Cluster	-39.7	-17.7	-2.4	650	~ 47	Stern et al. (1995)
IC2391 Super Cluster	-20.6	-15.7	-9.1	35–55	~ 155	Barrado y Navascués et al. (1999)
Pleiades Open Cluster	-11.6	-21	-11.4	120	120–140	Stauffer et al. (1998)
Tucana/Horologium	-11	-21	0	30	25–80	Torres et al. (2008)
TW Hydrae Association	-12	-19	-8	8–10	20–120	Mentuch et al. (2008); Torres et al. (2008)
Ursa Majoris Moving Group	14.9	1	-10.7	300	~ 25	Zuckerman & Song (2004); King & Schuler (2005)

Table 5. Kinematics and Young Moving Group Memberships

Name	SpT	Dist ^a	U	V	W	Δv^b	$\tilde{\chi}^2$	Prob. of Kinematic Match	Kin. ^c YMG Match	YMG Age Myr	Ages ^d from SLR09 Myr	Quality ^e of Match
	M–		km s ^{−1}	km s ^{−1}	km s ^{−1}	km s ^{−1}						
2MASS J00034227-2822410	7.0	π	-27.2 ± 4.8	-40.3 ± 3.6	-19.2 ± 1.4	–	–	–	–	–	300-1000	–
G 217-32 (AB)	3.8	phot	-20.8 ± 4.3	-8.2 ± 2.3	-5.6 ± 0.9	–	–	–	–	–	35-300	–
LP 348-40	3.5	phot	11.6 ± 2.3	-41.3 ± 1.9	19.1 ± 2.5	–	–	–	–	–	$\gtrsim 2000$	–
NLTT 614	6.4	phot	-18.8 ± 3.1	-6.5 ± 1.7	-0.9 ± 0.8	–	–	–	–	–	90-300	–
1RXS J001557.5-163659 (AB)	4.1	π	9.1 ± 0.9	11.2 ± 0.9	-18.8 ± 0.8	–	–	–	–	–	35-300	–
GJ 1006 A	3.6	π	-21.1 ± 13.2	-91.4 ± 10.2	-42.2 ± 10.7	–	–	–	–	–	35-300	–
GJ 3030	2.4	phot	-15.4 ± 7.9	-21.9 ± 4.6	-3.7 ± 1.8	5.3	0.5	–	Car	30	20-150	BBA
GJ 3036 (AB)	3.7	phot	-34.9 ± 9.0	-11.1 ± 5.4	6.0 ± 3.1	–	–	–	–	–	35-300	–
NLTT 1875	4.3	phot	-23.2 ± 5.2	-15.5 ± 3.2	-3.6 ± 1.0	6.1	6.3	–	IC2391	35–55	40-300	BBA
G 69-32	4.6	π	-38.0 ± 1.2	-16.9 ± 0.8	-1.9 ± 0.5	1.9	0.7	87%	Hyades	625	60-300	ABA
G 132-51 B (W)	2.6	π	-5.7 ± 1.2	-26.4 ± 1.0	-16.6 ± 1.6	3.5	2.1	56%	ABDor	50–100	20-150	AAA
G 132-51 B (E)	3.8	π	-5.5 ± 1.2	-26.6 ± 1.0	-16.5 ± 1.6	3.5	2.1	55%	ABDor	50–100	35-300	AAA
G 269-153 A (NE)	4.3	π	-9.5 ± 2.5	-26.1 ± 2.5	-14.8 ± 2.6	1.9	0.4	95%	ABDor	50–100	40-300	AAA
G 269-153 B (SW)	4.6	π	-9.5 ± 2.5	-26 ± 2.4	-13.8 ± 1.1	1.8	0.3	95%	ABDor	50–100	60-300	AAA
G 269-153 C (E)	5.0	π	-7.7 ± 2.5	-24.9 ± 2.4	-13.9 ± 0.6	2.2	0.5	93%	ABDor	50–100	–	AAA
G 172-56	5.4	phot	-21.6 ± 2.4	-2.8 ± 1.9	-1.8 ± 0.7	–	–	–	–	–	60-300	–
2MASS J01351393-0712517	4.3	π	-12.6 ± 2.7	-15.4 ± 2.1	-10.8 ± 4.9	2.1	0.3	96%	β Pic	10–12	40-300	AAB ^f
G 271-110	3.5	π	-13.2 ± 1.1	-19.2 ± 1.2	-11.8 ± 0.6	2.4	1.1	77%	Pleiades	120	25-300	ABA
1RXS J015027.1-185134	5.4	π	17.2 ± 3.1	-38.4 ± 3.9	-25.0 ± 0.9	–	–	–	–	–	60-300	–
NLTT 6549 (AB)	1.5	phot	-42.5 ± 13.1	-21.4 ± 11.5	0.7 ± 5.9	5.6	0.4	–	Hyades	625	15-150	BBB
GJ 1041 A (SW)	0.6	π	-16.1 ± 1.7	-16.8 ± 1.5	14.7 ± 0.7	7.2	7.9	5%	Her-Lyr	200	–	BAA
GJ 1041 Bab (NE)	2.2+3.0	–	–	–	–	–	–	–	Her-Lyr	200	–	–
GJ 82	4.2	π	-8.7 ± 0.7	-21.2 ± 0.6	-5.2 ± 0.6	2.5	1.4	71%	Car	30	35-300	ABA
GJ 3136	2.9	phot	-8.0 ± 5.0	-23.8 ± 5.4	-12.7 ± 8.0	3.4	0.3	–	ABDor	50–100	20-300	BAA
1RXS J021836.6+121902	1.9	phot	-26.3 ± 4.5	-15.2 ± 5.1	-20.9 ± 3.4	–	–	–	–	–	20-150	–
GJ 3150	3.6	phot	-28.3 ± 5.0	-15.6 ± 5.0	-4.6 ± 2.9	–	–	–	–	–	35-300	–
1RXS J022735.8+471021	4.6	phot	-2.8 ± 1.3	-15.6 ± 1.6	-8.0 ± 2.5	–	–	–	–	–	60-300	–
1RXS J023138.7+445640	4.4	phot	-0.5 ± 3.0	-8.9 ± 2.5	-1.4 ± 1.6	–	–	–	–	–	40-300	–
G 36-26	5.9	phot	7.6 ± 1.4	-12.3 ± 3.5	-12.4 ± 4.0	–	–	–	–	–	90-300	–
GJ 3174	3.7	π	-23.6 ± 1.8	-39.1 ± 1.9	9.9 ± 1.3	–	–	–	–	–	35-300	–
LP 247-13	2.7	π	-41.4 ± 1.0	-19.1 ± 1.5	-2.2 ± 1.6	2.2	0.9	83%	Hyades ^g	625	20-100	AAB
G 246-33	4.1	phot	-24.4 ± 2.4	-4.7 ± 2.9	-1.5 ± 3.4	–	–	–	–	–	35-300	–
1RXS J032230.7+285852	4.0	π	-41.0 ± 0.7	-19.8 ± 1.2	-1.0 ± 1.1	2.8	1.6	67%	Hyades ^g	625	35-300	AAA

Table 5—Continued

Name	SpT	Dist ^a	U	V	W	Δv^b	χ^2	Prob. of Kinematic Match	Kin. ^c YMG Match	YMG Age Myr	Ages ^d from SLR09 Myr	Quality ^e of Match
	M–		km s ^{−1}	km s ^{−1}	km s ^{−1}	km s ^{−1}						
2MASS J03350208+2342356	8.5	π	-17.0 ± 1.8	-11.6 ± 2.1	-7.9 ± 2.0	7.1	6.7	8%	β Pic	10–12	10	BAA
1RXS J034231.8+121622	5.2	phot	-34.7 ± 1.2	-5.6 ± 1.8	-12.2 ± 1.7	–	–	–	–	–	60-300	–
G 80-21	2.8	π	-9.5 ± 0.8	-26.9 ± 1.0	-12.5 ± 0.8	2.1	1	81%	ABDor ^h	50–100	20-300	AAA
II Tau (SB1?)	4.6	π	-43.2 ± 0.8	-13.3 ± 1.8	-5.4 ± 1.7	6.3	6.5	9%	Hyades ^g	625	60-300	BAA
1RXS J041325.8-013919 (AB)	5.3	π	-30.3 ± 0.9	-17.5 ± 1.4	-7.1 ± 1.3	–	–	–	–	–	60-300	–
1RXS J041417.0-090650	4.3	π	-11.1 ± 1.0	-25 ± 1.3	-12.7 ± 1.1	3.9	2.9	41%	ABDor	50–100	10-40	AAA
GJ 3287	3.8	phot	-26.3 ± 2.4	-8.5 ± 3.2	-2.2 ± 3.8	–	–	–	–	–	35-300	–
GJ 3305 (AB)	1.1	π	-14.6 ± 0.9	-16.8 ± 1.4	-10.0 ± 1.2	4.1	3.4	34%	β Pic ^h	10–150	12	AAA
GJ 3304 A (SE)	4.6	π	-42.8 ± 1.4	-22.8 ± 2.1	13.7 ± 2.5	–	–	–	–	–	60-300	–
GJ 3304 B (NW)	5.0	–	–	–	–	–	–	–	–	–	–	–
NLTT 13728	6.0	π	-28.4 ± 0.3	-13.1 ± 0.3	-6.1 ± 0.3	–	–	–	–	–	10-90	–
NLTT 13837	4.3	π	21.6 ± 1.2	-5.9 ± 1.6	-17.8 ± 1.5	–	–	–	–	–	40-300	–
NLTT 13844	4.6	phot	-82.0 ± 2.9	-47.4 ± 8.9	-12.4 ± 8.7	–	–	–	–	–	60-300	–
2MASS J04465175-1116476 A (E)	4.9	π	-5.3 ± 0.7	-0.9 ± 1.2	-20.0 ± 1.2	–	–	–	–	–	60-300	–
2MASS J04465175-1116476 B (W)	6.0	π	-5.3 ± 0.7	-0.9 ± 1.2	-20.0 ± 1.2	–	–	–	–	–	–	–
2MASS J04472312-2750358	0.5	phot	-30.2 ± 2.1	-13.1 ± 1.5	-10.5 ± 1.0	–	–	–	–	–	$\gtrsim 400$	–
G 81-34 (AB)	4.0	phot	-30.3 ± 1.2	-7.9 ± 3.0	2.3 ± 3.2	–	–	–	–	–	35-300	–
1RXS J045101.0+312734	3.7	phot	-29.6 ± 0.8	-5.6 ± 2.4	4.4 ± 3.0	–	–	–	–	–	35-300	–
NLTT 14116	3.3	π	-9.1 ± 0.5	-29.5 ± 0.5	-13.3 ± 0.4	2.8	1.8	61%	ABDor ^h	50–100	25-300	AAA
GJ 3335	3.5	π	33.0 ± 1.6	-76.6 ± 4.9	-26.4 ± 3.5	–	–	–	–	–	25-300	–
NLTT 15049 A (SW)	3.8	π	-10.6 ± 1.3	-24.2 ± 1.4	-21.6 ± 1.0	–	–	–	–	–	35-300	–
NLTT 15049 B (NE)	5.0	π	-10.6 ± 1.3	-24.2 ± 1.4	-21.6 ± 1.0	–	–	–	–	–	–	–
GJ 207.1	2.0	π	-51.4 ± 5.5	-23.4 ± 13.4	-37.5 ± 16.3	–	–	–	–	–	20-150	–
1RXS J055446.0+105559	2.1	π	-11.6 ± 3.3	-2.9 ± 10.5	-20.6 ± 14.6	–	–	–	–	–	20-150	–
2MASS J05575096-1359503	7.0	π	–	–	–	–	–	–	–	–	2 ⁱ	–
GJ 3372 B	4.2	phot	-6.5 ± 1.9	-10.1 ± 2.9	-4.7 ± 1.5	6.8	6.6	–	Castor	200	40-300	BAA
G 249-36	4.9	phot	-123.9 ± 6.3	25.7 ± 8.9	39.8 ± 5.6	–	–	–	–	–	60-300	–
CD-35 2722	1.0	π	-7.5 ± 5.0	-27.5 ± 0.8	-14.6 ± 0.4	0.9	0.2	98%	ABDor ^h	50–100	–	AAA
GJ 3395	0.8	phot	-17.9 ± 2.6	-10.6 ± 6.6	-17.3 ± 5.0	–	–	–	–	–	20-150	–
G 108-36	2.5	π	-40.1 ± 0.4	-16.7 ± 0.7	-20.6 ± 1.0	–	–	–	–	–	20-150 ^d	–
GJ 3417 A (NE)	5.2	phot	-21.3 ± 4.0	-15.3 ± 6.4	15.2 ± 4.3	–	–	–	–	–	60-300	–
BD+20 1790	-1.0	π	-5.6 ± 0.8	-25.3 ± 1.4	-15.4 ± 0.8	3.3	2.2	54%	ABDor ^h	50–100	–	AAA
GJ 2060 A	1.3	π	-8.9 ± 0.7	-27.5 ± 1.2	-16.1 ± 0.4	2.3	1.3	73%	ABDor ^h	50–100	15-150	AAA

Table 5—Continued

Name	SpT	Dist ^a	U	V	W	Δv^b	$\tilde{\chi}^2$	Prob. of Kinematic Match	Kin. ^c YMG Match	YMG Age Myr	Ages ^d from SLR09 Myr	Quality ^e of Match
	M–		km s ^{−1}	km s ^{−1}	km s ^{−1}	km s ^{−1}						
GJ 2060 B	1.5	π	-8.9 ± 0.7	-27.5 ± 1.2	-16.1 ± 0.4	2.3	1.3	73%	ABDor	50–100	–	AAA
GJ 2060 C	5.0	π	-8.9 ± 0.7	-27.5 ± 1.2	-16.1 ± 0.4	2.3	1.3	73%	ABDor	50–100	–	AAA
GJ 277 B	3.3	π	-5.8 ± 0.3	-9.6 ± 0.8	-16.1 ± 0.7	–	–	–	J	–	25–300	–
1RXS J073829.3+240014	2.7	π	-20.7 ± 0.4	-9.1 ± 0.6	-11.1 ± 0.8	6.9	10.7	1%	IC2391	35–55	20–300	BBA
NLTT 18549	7.0	π	28.1 ± 0.8	-26 ± 1.8	-3.4 ± 1.3	–	–	–	–	–	10–100	–
2MASS J07572716+1201273	2.3	π	-20.9 ± 1.3	-37.7 ± 2.3	-14.4 ± 2.1	–	–	–	–	–	$\gtrsim 1200$	–
2MASS J08031018+2022154	3.3	phot	-33.3 ± 2.0	-15 ± 1.8	5.7 ± 2.7	–	–	–	–	–	25–300	–
GJ 316.1	6.0	π	-72.8 ± 1.4	-48.1 ± 1.2	-13.5 ± 1.8	–	–	–	–	–	100	–
NLTT 20303 A (W)	2.6	π	-22.8 ± 1.4	-15.7 ± 1.5	-8.3 ± 1.4	2.4	0.9	82%	IC2391	35–55	20–300	ABA
NLTT 20303 B (E)	3.5	π	-22.8 ± 1.4	-15.7 ± 1.5	-8.3 ± 1.4	2.4	0.9	82%	IC2391	35–55	–	ABA
LP 726-13	–	π	–	–	–	–	–	–	–	–	–	–
1RXS J091744.5+461229 (AB)	1.7	phot	-8.8 ± 4.2	-3.8 ± 1.7	-18.6 ± 4.3	–	–	–	–	–	20–150	–
G 43-2	2.0	π	-6.5 ± 0.5	16.4 ± 1.0	3.9 ± 0.4	–	–	–	–	–	20–150	–
NLTT 22741	4.5	phot	-11.3 ± 1.5	-17.3 ± 2.8	2.0 ± 1.2	4.3	2.0	–	TucHor	30	40–300	BBA
GJ 3577 A (W)	3.5	phot	-7.2 ± 3.7	-31.4 ± 9.4	-5.9 ± 3.1	–	–	–	–	–	25–300	–
G 196-3 A	3.0	phot	-4.7 ± 1.9	-10.8 ± 3.0	-2.3 ± 1.7	–	–	–	–	–	25–300	–
GJ 2079 (AB, SB1?)	0.7	π	-11.4 ± 0.7	-21.4 ± 0.8	-4.7 ± 0.5	2.0	0.9	83%	Car ^k	30	15–300 ^k	ABA
1RXS J101432.0+060649 A (E)	4.1	π	-24.0 ± 5.0	-24.8 ± 2.6	-8.5 ± 3.7	–	–	–	–	–	35–300	–
1RXS J101432.0+060649 B (W)	4.5	π	-24.0 ± 5.0	-24.8 ± 2.6	-8.5 ± 3.7	–	–	–	–	–	–	–
GJ 388	3.5	π	-14.9 ± 0.2	-7.6 ± 0.1	3.8 ± 0.2	–	–	–	–	–	25–300	–
G 44-9	5.9	π	-40.6 ± 2.2	-17.1 ± 0.9	-12.9 ± 1.5	–	–	–	–	–	90–300	–
2MASS J10364483+1521394 A (N)	4.0	π	15.1 ± 1.2	2.4 ± 1.0	-7.4 ± 0.7	3.6	2.9	42%	UMa	300	35–300	AAA
2MASS J10364483+1521394 Bab (S)	4.5+4.5	π	15.1 ± 1.2	2.4 ± 1.0	-7.4 ± 0.7	3.6	2.9	42%	UMa	300	35–300	AAA
GJ 3629 (AB)	3.0	phot	-20.8 ± 5.2	-11.8 ± 2.5	3.5 ± 2.7	–	–	–	–	–	25–300	–
GJ 3639	3.5	phot	-11.1 ± 4.5	-2.8 ± 1.8	-16.0 ± 2.1	–	–	–	–	–	25–300	–
NLTT 26114	3.0	π	-9.4 ± 0.7	7.1 ± 0.4	-20.1 ± 0.3	–	–	–	–	–	25–300	–
G 119-62	3.5	phot	-10.5 ± 2.4	2.7 ± 2.1	-1.5 ± 1.0	–	–	–	–	–	25–300	–
1RXS J111300.1+102518	3.0	π	21.5 ± 1.4	-0.5 ± 1.4	-14.4 ± 1.0	7.7	10.4	2%	UMa	300	25–300	BAA
GJ 3653	0.5	phot	-17.5 ± 8.6	-25.5 ± 6.0	-9.7 ± 4.2	7.6	1.1	–	Pleiades	120	15–150	BBA
2MASS J11240434+3808108	4.5	phot	13.0 ± 1.9	2.1 ± 1.0	-7.4 ± 0.8	3.9	3.0	–	UMa	300	40–300	BAA
G 10-52	3.5	π	20.6 ± 1.2	-3.4 ± 1.2	-11.4 ± 0.9	7.2	9.6	2%	UMa	300	25–300	BAA
G 122-74	3.5	phot	–	–	–	–	–	–	–	–	$\gtrsim 2000$	–
GJ 3729 (AB)	3.5	phot	-4.5 ± 4.8	-22.9 ± 5.1	1.4 ± 1.4	6.9	2.0	–	TucHor	30	25–300	BBA

Table 5—Continued

Name	SpT	Dist ^a	U	V	W	Δv^b	$\tilde{\chi}^2$	Prob. of Kinematic Match	Kin. ^c YMG Match	YMG Age Myr	Ages ^d from SLR09 Myr	Quality ^e of Match
	M–		km s ^{−1}	km s ^{−1}	km s ^{−1}	km s ^{−1}						
GJ 3730	4.0	π	-12.5 ± 1.3	-6.9 ± 1.1	-23.8 ± 0.2	—	—	—	—	—	35-300	—
1RXS J124147.5+564506	2.5	phot	17.0 ± 5.6	5.7 ± 3.6	-7.1 ± 0.7	6.2	4.2	—	UMa	300	20-150	BAB
GJ 490 B (ab)	4.0	π	-11.7 ± 1.3	-24.1 ± 1.1	-3.2 ± 0.5	4.5	4.3	24%	TucHor	30	35-300	ABA
GJ 490 A	0.5	π	-11.8 ± 1.2	-23.7 ± 1.0	-0.4 ± 0.6	2.9	1.6	65%	TucHor	30	15-150	ABA
NLTT 32659 A (W)	1.6	phot	-24.6 ± 10.2	-39.8 ± 8.0	-3.0 ± 1.7	—	—	—	—	—	20-150	—
NLTT 32659 B (E)	3.7	phot	—	—	—	—	—	—	—	—	35-300	—
GJ 1167 A	4.8	phot	-7.9 ± 4.2	-19.1 ± 3.7	-3.5 ± 2.6	4.6	1.2	—	Car	30	60-300	BBB
GJ 3786 (AB)	3.5	π	-34.7 ± 2.2	-43.7 ± 1.8	-0.5 ± 0.9	—	—	—	—	—	25-300	—
2MASS J13292408-1422122	2.8	phot	9.3 ± 2.3	4.7 ± 1.9	-5.8 ± 0.9	—	—	—	—	—	20-150	—
2MASS J14215503-3125537 (AB)	3.9	π	-39.5 ± 1.4	-12.2 ± 1.5	-8.5 ± 1.2	—	—	—	—	—	35-300	—
2MASS J1442809-0424078	3.0	phot	20.8 ± 4.2	0 ± 5.3	-7.6 ± 3.6	6.7	2.2	—	UMa	300	20-150	BAB
1RXSJ150907.2+590422	2.2	phot	14.4 ± 3.6	2.6 ± 3.3	-7.6 ± 2.7	3.6	1.1	—	UMa	300	20-150	BAB
GJ 9520	1.0	π	0.6 ± 0.3	9.7 ± 0.2	4.6 ± 0.4	—	—	—	—	—	15-150	—
NLTT 40561	3.5	phot	31.0 ± 7.9	-14.2 ± 6.8	4.3 ± 1.6	—	—	—	—	—	25-300	—
G 167-54	4.1	phot	-38.5 ± 3.7	-11.2 ± 3.3	-22.0 ± 1.7	—	—	—	—	—	$\gtrsim 4500$	—
2MASS J15534211-2049282 A (S)	3.4	π	-5.0 ± 7.5	-33 ± 16.9	-17.2 ± 15.5	7.5	0.3	96%	ABDor	50–100	3	BBB
GJ 3928 (AB)	5.3	phot	-13.7 ± 2.3	-10.7 ± 2.5	-6.3 ± 2.1	5.3	3.0	—	Castor	200	60-300	BAA
NLTT 43695 (E)	4.6	phot	-33.2 ± 3.2	-21.5 ± 1.9	-15.6 ± 1.4	—	—	—	—	—	60-300	—
LP 331-57 (AB)	2.4	phot	-7.3 ± 2.9	9.2 ± 3.9	-14.1 ± 4.9	—	—	—	—	—	20-150	—
2MASS J17073334+4301304	10.0	phot	—	—	—	—	—	—	—	—	—	—
GJ 669 B (W)	5.6	π	-36.9 ± 1.0	-19.4 ± 0.8	-2.3 ± 0.7	3.3	2.2	53%	Hyades	625	90-300	ABA
GJ 669 A (E)	3.4	π	-36.8 ± 0.9	-19.4 ± 0.7	-2.9 ± 0.6	3.4	2.5	48%	Hyades	625	25-300	ABA
1RXS J173130.9+272134	10.0	phot	—	—	—	—	—	—	—	—	20-300	—
G 227-22	6.1	phot	8.4 ± 5.5	2 ± 1.5	-5.0 ± 2.6	—	—	—	—	—	90-300	—
GJ 4044	4.5	π	-4.7 ± 0.5	0.3 ± 0.5	-19.5 ± 0.8	—	—	—	—	—	40-300	—
1RXS J183203.0+203050 A (N)	4.9	phot	9.9 ± 2.9	-30 ± 2.0	-9.6 ± 1.8	—	—	—	—	—	60-300	—
1RXS J183203.0+203050 B (S)	5.1	phot	9.1 ± 3.0	-30.9 ± 2.2	-9.9 ± 2.1	—	—	—	—	—	60-300	—
1RXS J184410.0+712909 A (E)	3.9	phot	-11.7 ± 3.3	-19.5 ± 3.1	-9.0 ± 1.9	1.1	0.1	—	TWA	8–10	35-300	BBB
1RXS J184410.0+712909 B (W)	4.1	phot	-11.9 ± 3.3	-18.3 ± 1.7	-8.3 ± 1.4	0.8	0.1	—	TWA	8–10	35-300	BBB
GJ 9652 A (SB1?)	4.5	π	-19.6 ± 1.9	-12 ± 1.6	66.5 ± 2.8	—	—	—	—	—	60-300	—
2MASS J19303829-1335083	6.0	π	-40.9 ± 0.8	38.2 ± 1.8	5.8 ± 1.3	—	—	—	—	—	90-300	—
1RXS J193124.2-213422	2.4	π	-24.3 ± 1.8	-16.8 ± 1.6	-2.4 ± 1.4	7.7	9.5	2%	IC2391	35–55	20-150	BBA
1RXS J193528.9+374605 (SB1?)	3.0	phot	-3.5 ± 2.0	-34.1 ± 0.9	-1.1 ± 2.5	—	—	—	—	—	20-300	—

Table 5—Continued

Name	SpT	Dist ^a	U	V	W	Δv^b	$\bar{\chi}^2$	Prob. of Kinematic Match	Kin. ^c YMG Match	YMG Age Myr	Ages ^d from SLR09 Myr	Quality ^e of Match
	M–		km s ^{−1}	km s ^{−1}	km s ^{−1}	km s ^{−1}						
1RXS J194213.0-204547	5.1	π	0.9 ± 0.3	-10 ± 0.6	-1.9 ± 0.5	—	—	—	—	—	60-300	—
G 125-36	2.1	phot	-45.3 ± 4.0	-13.6 ± 1.5	0.5 ± 3.3	7.5	4.7	—	Hyades	625	$\gtrsim 1200$	BBB
2MASS J20003177+5921289 (AB)	4.1	phot	11.6 ± 2.4	-6.4 ± 1.1	5.9 ± 2.9	—	—	—	—	—	35-300	—
1RXS J204340.6-243410 A (NE)	3.7	π	-7.5 ± 1.2	-8.5 ± 1.7	-5.4 ± 1.5	5.3	4.8	19%	Castor	200	35-300	BAA
1RXS J204340.6-243410 B (SW)	4.1	π	-8.2 ± 1.3	-8.7 ± 1.7	-4.9 ± 1.5	5.5	4.8	19%	Castor	200	35-300	BAA
NLTT 49856	4.5	π	-40.0 ± 0.6	-18.9 ± 0.4	-8.2 ± 0.7	6	7.9	5%	Hyades	625	40-300	BBA
2MASS J20530910-0133039	5.6	π	-35.7 ± 1.0	-39.3 ± 0.8	-12.3 ± 1.0	—	—	—	—	—	90-300	—
NLTT 50066 (AB)	2.9	π	-47.2 ± 3.4	-21.6 ± 1.1	-5.2 ± 4.0	—	—	—	—	—	20-300	—
GJ 4185 B	3.3	π	-16.5 ± 1.2	-1.3 ± 0.4	-10.4 ± 1.2	—	—	—	—	—	25-300	—
GJ 4185 A (ab)	3.3	π	-15.9 ± 1.2	-1.1 ± 0.6	-11.0 ± 1.2	—	—	—	—	—	25-300	—
GJ 4231	2.4	π	-7.5 ± 2.8	-28.5 ± 2.6	-14.0 ± 2.6	1.6	0.2	97%	ABDor	50–100	20-150	AAA
1RXS J221419.3+253411 (AB)	4.3	π	-16.4 ± 1.5	-24.4 ± 0.5	-8.2 ± 1.1	4.7	4.2	24%	Col	30	40-300	ABA
GJ 4282 A (E)	2.5	phot	-18.4 ± 6.5	-5.1 ± 2.3	-5.4 ± 4.0	—	—	—	—	—	20-150	—
GJ 4282 B (W)	2.6	phot	-18.2 ± 6.3	-4.7 ± 2.0	-6.0 ± 3.9	—	—	—	—	—	20-150	—
2MASS J22344161+4041387	6.0	phot	6.4 ± 15.3	-10.5 ± 4.5	0.1 ± 14.9	—	—	—	—	—	~ 1	—
LP 984-92	4.5	π	-11.3 ± 1.1	-16.8 ± 0.9	-11.2 ± 0.7	2.5	1.3	72%	β Pic ^h	10–12	40–300	AAA
LP 984-91	4.0	π	-11.3 ± 1.1	-16.8 ± 0.9	-11.2 ± 0.7	2.5	1.3	72%	β Pic ^h	10–12	—	AAA
GJ 873	3.2	π	19.8 ± 0.2	3.4 ± 0.2	-1.9 ± 0.1	—	—	—	—	—	25-300	—
NLTT 54873	3.8	phot	-19.3 ± 3.4	-6 ± 1.4	1.2 ± 2.5	—	—	—	—	—	35-300	—
GJ 875.1	2.7	π	-28.1 ± 1.2	-13.4 ± 0.6	-17.1 ± 0.6	—	—	—	—	—	20-300	—
2MASS J22581643-1104170	2.7	π	-9.8 ± 1.6	1.6 ± 0.8	-20.7 ± 0.8	—	—	—	—	—	20-300	—
GJ 9809	0.3	π	-6.5 ± 0.7	-26.7 ± 0.5	-15.6 ± 0.5	2.2	1.1	77%	ABDor ^h	50–100	10-150	AAA
NLTT 56194	7.5	phot	-13.3 ± 3.2	-7.9 ± 1.3	-6.3 ± 1.4	4.2	2.4	—	Castor	200	100-300	BAA
NLTT 56566 (AB)	3.8	π	-31.6 ± 2.1	-11.8 ± 1.2	-2.7 ± 1.0	—	—	—	—	—	35-300	—
GJ 4338 B (ab)	4.2	π	-10.6 ± 5.2	-20.2 ± 2.3	-2.2 ± 1.9	7.7	12.5	0%	Col	30	40-300	BBA
GJ 4337 A	2.9	phot	-15.7 ± 8.2	-23.3 ± 3.6	-4.5 ± 3.0	3.2	0.4	—	Col	30	20-300	BBA
GJ 1290	3.4	phot	-31.6 ± 9.0	-15.4 ± 4.4	0.1 ± 2.9	—	—	—	—	—	25-300	—
1RXS J235005.6+265942	4.0	phot	-12.4 ± 3.3	-9.5 ± 2.7	-6.9 ± 2.0	3.6	1.4	—	Castor	200	35-300	BAA
G 68-46	4.0	phot	-14.1 ± 3.9	-12.5 ± 2.0	-7.1 ± 1.4	4.7	2.1	—	ChaNear	10	35-300	BBB
1RXS J235133.3+312720 (AB)	2.0	phot	-9.3 ± 8.0	-27.7 ± 4.5	-13.5 ± 6.1	1.5	0.0	—	ABDor	50–100	20-150	BAA
1RXS J235452.2+383129	3.1	phot	9.8 ± 3.2	7.6 ± 1.7	-6.1 ± 2.2	—	—	—	—	—	25-300	—
GJ 4381 (AB)	2.8	phot	17.1 ± 4.6	-1.4 ± 2.6	-8.6 ± 4.9	3.9	0.9	—	UMa	300	20-300	BAA
G 273-191 A (N)	1.9	π	-37.1 ± 4.9	-17.9 ± 2.7	1.0 ± 2.1	4.3	1.6	66%	Hyades	625	20-150	ABB

Table 5—Continued

Name	SpT	Dist ^a	U	V	W	Δv^b	$\tilde{\chi}^2$	Prob. of Kinematic Match	Kin. ^c YMG Match	YMG Age Myr	Ages ^d from SLR09 Myr	Quality ^e of Match
	M–		km s ^{−1}	km s ^{−1}	km s ^{−1}	km s ^{−1}						
G 273-191 B (S)	1.9	π	-37.1 ± 4.9	-17.9 ± 2.7	1.0 ± 2.1	4.5	0.4	94%	Hyades	625	20-150	ABB
G 130-31	5.6	phot	30.9 ± 2.5	-43.3 ± 1.7	14.9 ± 3.0	–	–	–	–	–	90-300	–

^aThe source of the distance measurement, trigonometric (π) or photometric (phot.).

^bVelocity modulus to YMG. See text for details.

^cYMG to which the target is kinematically linked. In several cases, stars have UVW velocities matching several YMGs and thus we further filter based on sky position and/or age limits. See Section 5.2.

^dAge limits based on spectroscopic data such as H α emission, lithium absorption and gravity indices with a 300-Myr upper limit set by X-ray emission. (See SLR09 for details. In Figure 3 of SLR09, there is plenty of scatter in the X-ray levels of proposed Hyades members, so it is possible for stars with SpTs later than \approx M3.5, the upper age limit could be closer to the age of the 650-Myr Hyades Cluster.)

^eThis quality flag scores three characteristics with an ‘A’ or ‘B’: (1) The quality of the kinematic match (‘A’ for having a trigonometric distance, velocity modulus < 8 km s^{−1}, and match probability $>50\%$, or ‘B’ for photometric distance and low match probability). (2) 3-D positional coincidence in the sky of the star (common RA, Dec and distance as the proposed YMG). (3) Age agreement with the spectroscopically determined ages. A star flagged with ‘AAA’ is an excellent YMG candidate member.

^fIt has been recently shown empirically, for at least the 12 Myr old β Pic moving group, that lower ages limits of individual stars based on the lack of lithium absorption systematically overestimates the stars age as compared to model isochrones (Yee & Jensen 2010). This would imply that the lower age limits may be even lower, perhaps even as low as ≈ 10 Myr.

^gRöser et al. (2011) identified these stars as Hyades members. LP-247-13 however is much younger than the cluster based on its observed low gravity. 1RXS J032230.7+285852 and II Tau have rough upper limits of 300 Myr based on the X-ray. However, SLR09 do show that many of the mid- and late-M Hyades members also exhibit strong fractional X-ray luminosities. Also, using a mean RV for the RV variable II Tau makes it a poor kinematic match to the Hyades cluster.

^hPreviously identified as YMG members. Zuckerman et al. (2004) identified the AB Dor members, except for CD-35 2722 identified by Wahhaj et al. (2011) and BD+20 1970 by López-Santiago et al. (2006). β Pic members were identified by Torres et al. (2006).

ⁱThe very small parallax of this target implies that it is a brown dwarf with an age of less than 2 Myr based on evolutionary models.

^jWe calculated D_{trig} consistent with Hipparcos’ parallax and UVW s equal to those presented in Montes et al. (2001), who assign this star membership of a Castor group. However, the vel. mod. and χ^2 of this star for the Castor group are 8.2 km s^{−1} and 15, respectively, excluding the star as member by our selection criteria.

^kSchlieder et al. (2012) reports this star to be a member of the BPMG using the RV from López-Santiago et al. (2010) which differs from ours. The spectrum

does not have any Li absorption giving a likely lower age limit of 15 Myr. Schlieder et al. (2012) also report variable, yet low, H α emission. We did not detect any emission in our spectrum.

Table 6. CAPSCam Visual Binaries

VB Name	Flux Ratio in $\approx I$ $\pm 5\%$	Sep. " ± 0.04	P.A. deg. $\pm 1^\circ$	Note
G 269-153 AB ^a	1.1	1.94	45	Observed UT20090909
"	1.1	2.05	48.9	Observed UT20101114
G 269-153 AC	2.58	37.7	78.4	Observed UT20101114
GJ 1041 ABab	1.29	4.07	55	B component is a SB (Shkolnik et al. 2010).
GJ 3304 AB	1.5	1.03	305	Daemgen et al. (2007) reports sep=0.78" and PA = 300°.
2M 0446 AB	1.93	1.59	279	
NLTT 15049 AB	3	0.47	56	
NLTT 20303 AB	2.81	7.44	89.4	NLTT 20303B may be a very tight binary. ^b
1RXS 1014 AB	1.2	2.02	271	
2M 1036 AB	1.7	0.96	160	
NLTT 32659 AB	8.4	2.87	89	
1RXS 2043 AB	1.007	1.48	217	
G273-191 AB	1.057	1.96	176	

^aThis target, also known as G 274-24, was observed by Daemgen et al. (2007).

Table 7. Binaries Resolved with Keck and Subaru Adaptive Optics Imaging

Target	UT Date of Observation (Y/M/D)	Instrument	Filter	Δmag
G 217-32 AB	2010/08/18	NIRC2	<i>H</i>	0.475 (0.011)
1RXS J001557.5–163659 AB	2011/08/20	NIRC2	<i>H</i>	0.06 (0.05)
G 132-50 AB ^a	2011/12/28	HiCIAO	<i>K_s</i>	2.37 (0.16)
NLTT 6549 AB	2011/08/20	NIRC2	<i>H</i>	1.45 (0.09)
G 81-34 AB	2011/01/27	HiCIAO	<i>K_s</i>	0.57 (0.02)
GJ 2079 AB	2011/03/25	NIRC2	<i>K_s</i>	1.88 (0.06) ^b
GJ 3629 AB	2011/03/25	NIRC2	<i>K_s</i>	2.875 (0.012) ^c
GJ 3729 AB	2011/06/21	NIRC2	<i>H</i>	0.65 (0.06)
GJ 490 Bab	2011/03/25	NIRC2	<i>K_s</i>	0.061 (0.011)
2MASS J14215503–3125537 AB	2011/03/25	NIRC2	<i>K_s</i>	0.10 (0.05)
2MASS J20003177+5921289 AB	2010/08/18	NIRC2	<i>H</i>	0.029 (\dots) ^d
NLTT 50066 AB	2010/08/18	NIRC2	<i>H</i>	0.11 (0.05)
GJ 4185 Aab	2011/06/21	NIRC2	<i>H</i>	0.37 (0.07)
1RXS J221419.3+253411 AB	2011/06/21	NIRC2	<i>H</i>	1.08 (0.05)
GJ 4338 Bab	2010/08/18	NIRC2	<i>H</i>	0.27 (0.06)
GJ 4381 AB	2011/08/20	NIRC2	<i>H</i>	1.469 (0.011)
1RXS J235133.3+312720 (AB) ^e	2011/06/21	NIRC2	<i>H</i>	5.68 (0.04)

Note. — Binary separations at the time of discovery range from $0''.04$ – $0''.65$. Details about the observations, including astrometry for the binaries, will be presented in Bowler et al. (in preparation).

^aG 132-50 AB is a common proper-motion companion to our spectroscopic targets G 132-51 B (E & W). Including G 132-51 A, makes this a quintuple system in the AB Dor Moving Group.

^bThe peak counts from the primary ($\sim 1.2 \times 10^4$ DN pix^{−1}) are in a regime where the NIRC2 pixel response is modestly nonlinear ($\sim 10\%$). Before measuring flux ratios we therefore corrected these frames using the response curve derived by S. Metchev (private communication).

^cThe age (~ 25 – 300 Myr) and distance (~ 22 pc) of this system implies that GJ 3629 B is a brown dwarf based on the evolutionary models of Burrows et al. (1997). The discovery of this substellar companion is presented in Bowler et al. (2012, ApJ, submitted).

^dFlux ratio measurement is from a single image.

^eDetails of this discovery are reported in Bowler et al. (2012).

Table 8. Radial Velocity Variable Targets

VB Name	RV km s ⁻¹	Ref.
II Tau	37.9 ± 0.2	this work
	43.1 ± 0.6	this work
GJ 2079 (AB)	29.3 ± 1.2	Mochnacki et al. (2002)
	17.2 ± 0.4	this work
	10.0 ± 1.0	Montes et al. (2001)
	2.7 ± 0.1	López-Santiago et al. (2010)
	4.9 ± 1.5	Gizis et al. (2002)
GJ 9652 A	-88.8 ± 1.1	this work
	-73.0 ± 0.8	this work
1RXS J193528.9+374605	-23.2 ± 0.2	this work
	-43.4 ± 0.3	this work